JCI The Journal of Clinical Investigation

Schwann cells expressing nociceptive channel TRPA1 orchestrate ethanol-evoked neuropathic pain in mice

Francesco De Logu, … , Pierangelo Geppetti, Romina Nassini

J Clin Invest. 2019. https://doi.org/10.1172/JCI128022.

Research In-Press Preview Neuroscience

Graphical abstract

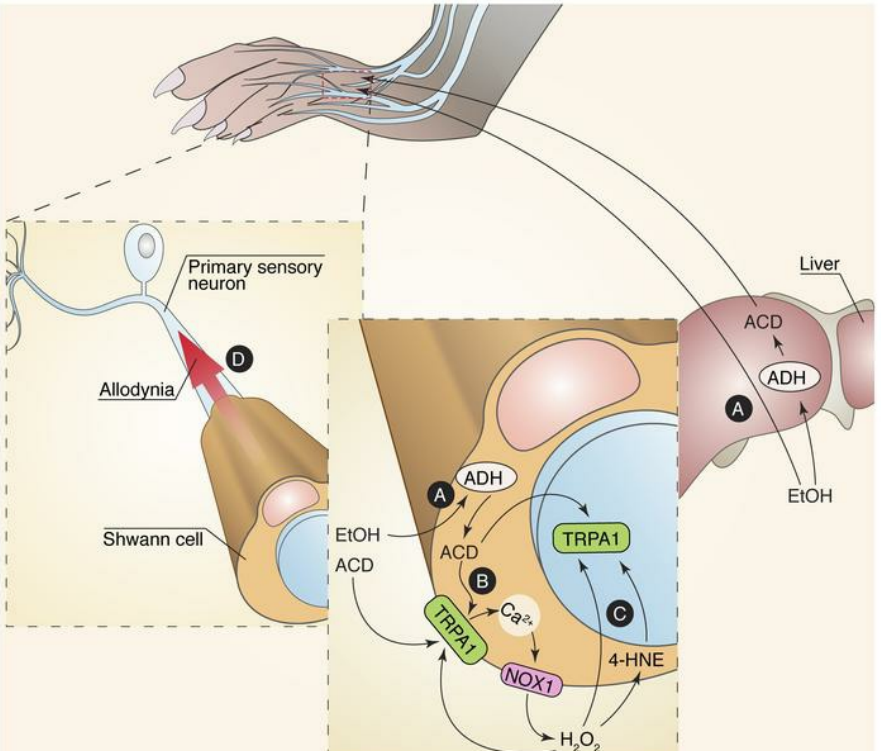

Find the latest version:

http://jci.me/128022/pdf

Schwann cells expressing nociceptive channel TRPA1 orchestrate ethanol-evoked neuropathic pain in mice

Francesco De Logu[1], Simone Li Puma[1], Lorenzo Landini[1], Francesca Portelli[2] Alessandro Innocenti[3], Daniel Souza Monteiro de Araujo[1,4], Malvin N. Janal[5], Riccardo Patacchini[6], Nigel W. Bunnett[7], Pierangelo Geppetti[1*], Romina Nassini[1]

[1]Department of Health Sciences, Section of Clinical Pharmacology and Oncology, University of Florence, Florence, Italy; [2]Department of Health Sciences, Histopathology and Molecular Diagnostics; University of Florence, Florence, Italy; [3]Plastic and Reconstructive Microsurgery, Careggi University Hospital, Florence, Italy; [4]Department of Neurobiology and Program of Neurosciences, Institute of Biology, Fluminense Federal University, Niterói, RJ, Brazil; [5]Department of Epidemiology and Health Promotion, New York University College of Dentistry, New York, USA; [6]Department of Corporate Drug Development, Chiesi Farmaceutici SpA, Parma, Italy; [7]Departments of Surgery and Pharmacology, Columbia University in the City of New York, USA.

*** Corresponding Author**

Pierangelo Geppetti, MD

Department of Health Sciences, University of Florence

Viale Pieraccini 6, 50139 Florence, Italy

geppetti@unifi.it

Mobile: +39 349 271 0476

Conflict of interest. RP is fully employed at Chiesi Farmaceutici SpA, Parma, Italy. NWB is a founding scientist of Endosome Therapeutics Inc. The other authors declare no competing financial interests.

Abstract

Excessive alcohol consumption is associated with spontaneous burning pain, hyperalgesia and allodynia. Although acetaldehyde has been implicated in the painful alcoholic neuropathy, the mechanism by which the ethanol metabolite causes pain symptoms is unknown. Acute ethanol ingestion caused delayed mechanical allodynia in mice. Inhibition of alcohol dehydrogenase (ADH) or deletion of transient receptor potential ankyrin 1 (TRPA1), a sensor for oxidative and carbonyl stress, prevented allodynia. Acetaldehyde generated by ADH in both liver and Schwann cells surrounding nociceptors was required for TRPA1-induced mechanical allodynia. *Plp1-Cre;Trpa1*$^{fl/fl}$ mice with a tamoxifen-inducible specific deletion of TRPA1 in Schwann cells revealed that channel activation by acetaldehyde in these cells initiates a NADPH oxidase-1 (NOX-1)-dependent production of hydrogen peroxide (H_2O_2) and 4-hydroxynonenal (4-HNE), which sustains allodynia by paracrine targeting of nociceptor TRPA1. Chronic ethanol ingestion caused prolonged mechanical allodynia and loss of intraepidermal small nerve fibers in WT mice. While *Trpa1*$^{-/-}$ or *Plp1-Cre*;*Trpa1*$^{fl/fl}$ mice did not develop mechanical allodynia, they did not show any protection from the small fiber neuropathy. Human Schwann cells express ADH/TRPA1/NOX1 and recapitulate the proalgesic functions of mouse Schwann cells. TRPA1 antagonists might attenuate some symptoms of alcohol-related pain.

Keywords

TRPA1, ethanol, Schwann cells, oxidative stress, neuropathic pain

Introduction

Alcohol abuse and dependence are among the major healthcare problems in the world (1). The impact of alcohol abuse continues to grow due to the rising incidence of excessive drinking by women and young people (2). Nevertheless, the male/female ratio of current drinkers and heavy episodic drinkers, which is 1.7 and 2.5, respectively, indicate twice the prevalence in men compared to women (2). About 60% of alcoholics exhibit a peripheral polyneuropathy, associated with pain and dysesthesias of the lower extremities (3). Reduced thiamine levels (4), which cause peripheral neuropathy in patients with post-gastrectomy polyneuropathy or beriberi, have been reported in alcoholics, and have been considered responsible for the peripheral neuropathy (5, 6). However, the observation that painful polyneuropathy is present in alcoholics with normal thiamine status (6), and that the clinical and pathological features of alcoholic neuropathy are distinct from those associated with thiamine deficiency (7) led to the conclusion that alcohol exerts a direct toxic effect on peripheral nerves. However, the mechanism by which ethanol targets peripheral nerves to cause the painful condition remains unknown.

Alcohol dehydrogenase (ADH) converts ethanol into the reactive and toxic product acetaldehyde, which is rapidly metabolized to acetic acid by the mitochondrial aldehyde dehydrogenase-2 (ALDH2) (8). Acetaldehyde is considered as the major contributor of the detrimental effects produced by acute and chronic alcohol consumption, including flushing, headache, cirrhosis and cancer (9-12). Mutations of the ADH and ALDH2 genes, which respectively accelerate ethanol conversion to acetaldehyde and slow down acetaldehyde metabolism, make East Asians susceptible to alcohol-induced symptoms with lower rates of alcohol use (13, 14). Acetaldehyde generates advanced glycation end-products and increases oxidative stress, which can contribute to ethanol-induced painful

neuropathy (15). In particular, preclinical studies and clinical evidence have implicated acetaldehyde in the genesis of the neuronal damage associated with ethanol consumption (3). However, the pathways by which acetaldehyde causes ethanol-evoked neuropathic pain are poorly understood.

Elevated local concentrations (1-3%) of ethanol have been shown to activate the transient receptor potential vanilloid 1 (TRPV1) channel on primary sensory nerves to induce pain and neurogenic inflammation (16). A related channel, TRP ankyrin 1 (TRPA1), is uniquely sensitive to multiple ROS, reactive nitrogen (RNS) and carbonyl (RCS) species (17-19). Saturated and unsaturated aldehydes, including acetaldehyde and 4-hydroxynonenal (4-HNE), also activate TRPA1 to cause pain-like responses (20, 21). TRPV1, TRPA1 and other TRP channels, including the vanilloid 4 (TRPV4), are expressed by a subpopulation of primary sensory neurons that signal pain (19). In the present study, we explored the role of TRP channels in the pain-like responses evoked by acute and chronic ethanol ingestion in mice.

We found that local (intraplantar) injection of ethanol in the mouse hind paw caused an acute nociceptive response due to direct activation of TRPV1, as previously reported (16). In addition, ethanol (either intraplantar or intragastric) caused a delayed and prolonged TRPV1-independent mechanical allodynia of the hind paw that was prevented by ADH and TRPA1 inhibition. Surprisingly, Schwann cells that ensheath plantar nerve fibers expressed ADH, which mediated the local conversion of ethanol to acetaldehyde. Selective deletion of TRPA1 on Schwann cells or nociceptors revealed that acetaldehyde, generated in the liver or locally, activates TRPA1 on Schwann cells (22) to produce oxidative and carbonylic stress, which target neuronal TRPA1 to sustain allodynia. Notably, mice fed daily with an ethanol-containing diet, which mimics chronic alcohol ingestion by alcoholics, developed a prolonged allodynia that was associated with loss of intraepidermal nerve fibers (IENF). Allodynia caused by chronic ethanol ingestion

was prevented by the same genetic and pharmacological disruptions of TRPA1 and oxidative stress that attenuated allodynia evoked by acute ethanol exposure. Thus, TRPA1 antagonism might represent an effective treatment for pain in alcoholics.

Results

TRPV1 mediates acute nociception but not sustained allodynia to local administration of ethanol

To explore the mechanisms of alcohol-induced nociception, ethanol was administered locally to the hind paw of C57BL/6J mice. Injection of intraplantar ethanol (15-80% in 0.9% NaCl) caused dose-dependent immediate nociceptive behavior, which did not last more than 5 min (Figure 1A). Ethanol also produced a delayed and prolonged (1-6 h) mechanical allodynia (Figure 1B). The short-lived nociceptive response was absent in *Trpv1*$^{-/-}$ mice (Figure 1C), and in C57BL/6J mice pretreated with the TRPV1 antagonist, SB366791 (Supplementary Figure 1A), supporting previous evidence that ethanol selectively targets TRPV1 to signal acute pain (16). In contrast, TRPV1 deletion or antagonism did not affect ethanol-evoked mechanical allodynia (Figure 1D and Supplemental Figure 1B). Thus, whereas direct TRPV1 engagement mediates acute ethanol-evoked nociception, ethanol induces sustained mechanical allodynia by a TRPV1-independent mechanism. Ethanol-induced nociception and allodynia were similar in *Trpv4*$^{-/-}$ mice and in WT littermates (Supplementary Figure 1C and D).

Acetaldehyde and TRPA1 mediate sustained allodynia to local and intragastric administration of ethanol

ADH mediates the first step of alcohol metabolism, converting ethanol to the saturated aldehyde acetaldehyde, which can activate TRPA1 (20). We examined the contribution of ADH and TRPA1 to ethanol-evoked allodynia. Intragastric or intraplantar

pretreatment of C57BL/6J mice with 4-methylpyrazole (4-Mp), a selective ADH inhibitor, prevented ethanol-evoked allodynia (Figure 1E and F). The nociceptive response evoked by intraplantar ethanol observed in *Trpa1*$^{+/+}$ mice was also present in *Trpa1*$^{-/-}$ mice (Figure 1G). However, mechanical allodynia produced by intraplantar ethanol in *Trpa1*$^{+/+}$ mice was absent in *Trpa1*$^{-/-}$ mice (Figure 1H). Systemic (i.p.) or intraplantar administration of A967079, a TRPA1 antagonist, 2 h after ethanol reversed sustained allodynia (Supplementary Figure 1E and F). Intraplantar injection of acetaldehyde (1-20 nmol) into the hind paw of C57BL/6J mice replicated the actions of ethanol, causing a dose-dependent immediate and transient nociceptive response (Figure 1I), followed by a delayed and prolonged (1-8 h) allodynia (Figure 1J). Both responses were absent in *Trpa1*$^{-/-}$ mice (Figure 1K and L). Systemic (i.p.) or intraplantar administration of A967079 reversed immediate nociception and sustained allodynia evoked by intraplantar acetaldehyde in C57BL/6J mice (Supplementary Figure 1G-I). Furthermore, the acute nociceptive response and the delayed mechanical allodynia induced by intraplantar acetaldehyde in *Trpv1*$^{+/+}$ mice remained unaffected in *Trpv1*$^{-/-}$ mice (Supplementary Figure 1J and K). The results are consistent with the hypothesis that ethanol induces allodynia by a mechanism that entails metabolism to acetaldehyde, which activates TRPA1.

Examination of the responses evoked by local injection of ethanol or acetaldehyde provides mechanistic insights into alcohol-induced pain. However, the ingestion of alcohol causes peripheral neuropathy in alcoholics. To mimic these circumstances, we administered graded doses of ethanol (1-4 ml/kg of ethanol 15% in 0.9% NaCl) to mice by intragastric administration. Even at the highest dose (15%, 4 ml/kg, intragastric), ethanol did not induce acute nociception or affect motor coordination, evaluated using a rotarod: no falls were observed in mice receiving either vehicle (n=8) or ethanol (15%, 4 ml/kg, n=8). However, intragastric ethanol evoked a dose-related delayed and sustained

(1-6 h) mechanical allodynia in C57BL/6J mice and *Trpa1*$^{+/+}$ mice, but not in *Trpa1*$^{-/-}$ mice (Figure 2A and B). Ethanol-evoked mechanical allodynia was preserved in *Trpv1*$^{-/-}$ or *Trpv4*$^{-/-}$ mice (Supplementary Figure 1L and M). Systemic (i.p.) or intraplantar administration of A967079 to C57BL/6J mice reversed allodynia evoked by intragastric ethanol (Figure 2C and D).

After gavage, ethanol levels in plasma, liver and paw were maximal at 30 min, and declined to baseline at 3 h (Figure 2E), when mechanical allodynia was maximal (*e.g.*, Figure 2A). The temporal dissociation between ethanol levels in plasma and tissues and allodynia suggests that ethanol does not directly activate TRPA1 to cause allodynia. Administration of the ADH inhibitor 4-Mp (intragastric) before ethanol prevented allodynia (Figure 2F). These results suggest that acetaldehyde, but not ethanol, activates TRPA1 to initiate allodynia.

Schwann cell ADH converts ethanol to acetaldehyde in peripheral tissues

Ethanol is mainly converted to acetaldehyde by ADH in the liver. However, ADH is expressed in other tissues (23-26). We detected mRNAs encoding ADH1, ADH5 and ADH7 in homogenates of mouse paw (Figure 3A). ADH immunoreactivity was confined to the nerve trunk within the paw, where it was co-expressed with S100, a specific marker of Schwann cells, but not in PGP9.5-positive nerve fibers (Figure 3B and C and Supplementary Figure 2A). Exposure of cultured mouse Schwann cells to ethanol induced the generation of acetaldehyde, a response that was prevented by 4-Mp (Figure 3D). Local (intraplantar) administration of ethanol to the paw also resulted in increased paw tissue levels of acetaldehyde within 15 min (Figure 3E). The local (intraplantar) administration of 4-Mp inhibited acetaldehyde formation (Figure 3F) and allodynia (Figure 1F) induced by intraplantar ethanol. The effects of intragastric ethanol on allodynia and acetaldehyde levels were partially reduced by pretreatment with

intraplantar (Figure 3G and H), or completely attenuated by, intragastric 4-Mp (Figure 3H and 2F). These results suggest that Schwann cells in the paw express ADH and convert ethanol to acetaldehyde. This local generation to acetaldehyde, together with the hepatic generation of acetaldehyde, can cause TRPA1-dependent sustained allodynia.

Acetaldehyde via TRPA1 generates ROS that sustain ethanol-evoked allodynia

To strengthen the hypothesis that acetaldehyde initiates allodynia by activating TRPA1, we treated mice with systemic (0.1-1 mg/kg, i.p.) acetaldehyde. Acetaldehyde (i.p.) did not affect motor coordination, as no falls was observed with either vehicle (n=8) or acetaldehyde (1 mg/kg, n=8). Acetaldehyde (i.p.) did not cause detectable acute nociceptive behavior, but evoked a dose-dependent, delayed and prolonged (1-8 h) mechanical allodynia in C57BL/6J mice (Figure 4A). Acetaldehyde did not cause allodynia in *Trpa1*$^{-/-}$ mice (Figure 4B). Systemic (i.p.) and intraplantar A967079 prevented acetaldehyde-evoked allodynia in C57BL/6J mice (Figure 4C and D). However, acetaldehyde formation in liver and paw after intragastric ethanol did not coincide with allodynia (Figure 4E); the levels of acetaldehyde in the liver and paw had returned to baseline by 3 h after intragastric ethanol (Figure 4E), when allodynia was robustly maintained (Figure 2A). Furthermore, administration of the ADH inhibitor 4-Mp (intragastric) after ethanol did not affect allodynia (Figure 4F). These results suggest the existence of additional mechanisms of ethanol-induced allodynia.

Both ethanol and acetaldehyde can release ROS (27-29). ROS and their carbonylic byproducts, including 4-HNE, activate TRPA1 (17, 21). To examine the contribution of ROS to ethanol-evoked allodynia, we treated mice with the ROS scavenger, phenyl-α-tert-butyl nitrone (PBN). PBN (i.p. or intraplantar) reversed the allodynia evoked by ethanol (both intraplantar and intragastric) (Figure 4G and H; Supplementary Figure 3A and B) or acetaldehyde (Figure 4I and J; Supplementary Figure 3C and D). Ethanol

(intragastric or intraplantar) increased H_2O_2 and 4-HNE levels in the paw (Figure 5A and B). However, while H_2O_2 levels were elevated for 3 h, 4-HNE content, measured by either immunofluorescence or by a biochemical assay, persisted for 6 h (Figure 5A and B). To test the hypothesis that the late phase of allodynia was mainly due to RCS, N-acetyl cysteine (NAC), which efficiently scavenges α,β-unsaturated aldehydes, including 4-HNE (30), was given (i.p.) to mice 5 h after ethanol (intragastric). NAC (i.p.) attenuated mechanical allodynia at 6 h (Figure 5C). These results suggest that carbonylic derivatives, which are more stable and longer acting than ROS (30), sustain the final phase of allodynia. To support this hypothesis, PBN, which selectively scavenges ROS, was ineffective in the final phase of allodynia (Figure 5C).

Administration of the ADH inhibitor 4-Mp (Figure 5D) or the ROS scavenger, PBN (Figure 5E), blunted the ethanol-induced increase in H_2O_2 levels. Acetaldehyde (i.p. or intraplantar) increased H_2O_2 in paw tissue (Figure 5F), an effect that was inhibited by PBN (Figure 5G). Surprisingly, we observed that pharmacological blockade or genetic deletion of TRPA1 attenuated both ethanol- and acetaldehyde-evoked increases in H_2O_2 in the paw (Figure 5E and 5G-I). We have recently reported the presence of different NOX isoforms in Schwann cells of the mouse sciatic nerve, where they co-localize with TRPA1 to increase oxidative stress (22). Here, we observed that Schwann cells of plantar nerve fibers expressed NOX1 and TRPA1 (Figure 6A and B and Supplementary Figure 2A). A NOX1 antagonist (ML171, i.p.) reversed allodynia evoked by ethanol (intragastric) and acetaldehyde (i.p.) (Figure 6C).

Our results suggest that ADH in the liver or in Schwann cells of the sciatic nerve converts ethanol to acetaldehyde; Schwann cell-derived acetaldehyde might activate TRPA1 in an autocrine manner to generate ROS and RCS, which could amplify and sustain allodynia. To specifically define the role of Schwann cell TRPA1 in ethanol-evoked nociception, we studied mice with Schwann cell-specific deletion of TRPA1.

Mice with conditional ablation of TRPA1 in Schwann cells (*Plp1-Cre^{ERT};Trpa1$^{fl/fl}$*) (22) exhibited a normal acute nociception after intraplantar ethanol or AITC (TRPA1 agonist) (Supplementary Figure 4A). As these two responses are mediated by neuronal TRPV1 and TRPA1, respectively, the results indicate that the neuronal channel is unaffected by deletion of Schwann cell TRPA1. However, allodynia and generation of H_2O_2 in the paw evoked by intraplantar or intragastric ethanol were attenuated in *Plp1-Cre^{ERT};Trpa1$^{fl/fl}$* mice (Figure 6D and E).

To further support the involvement of Schwann cell TRPA1 in ethanol-evoked mechanical allodynia, mice were locally treated with the TRPA1 antisense oligonucleotide (TRPA1 AS-ODN) or its mismatched (TRPA1 MM-ODN) analogue (both intraplantar) (Supplementary Figure 4C) or with the activated form of tamoxifen (4-hydroxytamoxifen, 4-OHT) (intraplantar) (Supplementary Figure 4G). Both treatments were given by injection in the vicinity of the plantar nerve trunk, before ethanol (intraplantar or intragastric). In mice treated with TRPA1 AS-ODN or 4-OHT, acute nociception responses by intraplantar ethanol or AITC (dependent on neuronal TRPV1 and TRPA1, respectively) were preserved (Supplementary Figure 4E and I), indicating that neuronal TRPV1 and TRPA1 were unaffected. However, colocalization of TRPA1 with the Schwann cell marker, S-100, in the plantar nerve was markedly reduced (Supplementary Figure 4D and H), confirming selective deletion of TRPA1 in Schwann cells. After intragastric ethanol, mechanical allodynia was attenuated solely in the paw treated with the TRPA1 AS-ODN, while it was unaffected in the TRPA1 MM-ODN treated paw (Supplementary Figure 4F). Similar results were obtained with local treatment with 4-OHT. Notably, 4-OHT attenuated mechanical allodynia evoked by intragastric ethanol only on the paw treated with 4-OHT, but not in the contralateral paw (Supplementary Figure 4J). These data support the hypothesis that ethanol-evoked allodynia is initiated and maintained by Schwann cell TRPA1.

To specifically investigate the contribution of neuronal TRPA1, we studied mice with selective deletion of TRPA1 in primary sensory neurons (*Adv-Cre;Trpa1$^{fl/fl}$*) (31). AITC-induced nociception was attenuated in *Adv-Cre;Trpa1$^{fl/fl}$* mice, which confirms deletion of the functional channel (Supplementary Figure 4B). In *Adv-Cre;Trpa1$^{fl/fl}$* mice, ethanol-induced acute nociception was preserved (Supplementary Figure 4B). However, whereas allodynia evoked by intragastric or intraplantar ethanol was attenuated, H_2O_2 formation was unaffected (Figure 6F and G). Thus, in contrast with the Schwann cell channel, TRPA1 expressed by nociceptor signals pain, but does not contribute to oxidative stress generation.

Chronic ethanol ingestion evokes ROS formation and allodynia dependent on Schwann cell TRPA1

In WT mice, daily ingestion of an ethanol (5% for 28 d) containing diet (32) induced a progressively increasing mechanical allodynia that was apparent at 5-8 d, stabilized after two wk and maintained for the entire period of observation (Figure 7A and B). Both *Trpa1$^{-/-}$* and *Plp1-Cre^{ERT};Trpa1$^{fl/fl}$* mice were protected from the development of allodynia (Figure 7B). At day 28 after the initiation of the ethanol diet, the allodynia observed in WT mice was reversed by treatment (i.p.) with the TRPA1 antagonist, A967079, or with the ROS scavenger, PBN (Figure 7C). At day 28, WT mice showed increased levels of H_2O_2 and 4-HNE in the plantar nerve that were attenuated in *Trpa1$^{-/-}$* and *Plp1-Cre^{ERT};Trpa1$^{fl/fl}$* mice (Figure 7D). However, the loss of PGP9.5 positive IENF observed at day 28 was unaffected in either *Trpa1$^{-/-}$* or *Plp1-Cre^{ERT};Trpa1$^{fl/fl}$* mice (Figure 7E). At day 28, the levels of ethanol or ACD in the paw of *Trpa1$^{-/-}$* and *Plp1-Cre^{ERT};Trpa1$^{fl/fl}$* mice were not different from those measured in respective WT and control mice (Supplementary Figure 5A-D).

Ethanol evokes ADH- and TRPA1-dependent ROS formation by human Schwann cells

Our findings reveal an unexpected but critical role for Schwann cells in ethanol-evoked mechanical allodynia in mice. To assess whether these findings could translate to humans, we studied primary cultures of human Schwann cells (HSC) and Schwann cells in sections of human skin. HSC in culture expressed immunoreactive S100 and immunoreactive ADH (Figure 8A). In nerve bundles in biopsies of human skin, immunoreactive ADH colocalized with S100 (Figure 8B and Supplementary Figure 2B). mRNA encoding multiple isoforms of ADH (1A, 1B, 1C and 5) was amplified from HSC in culture (Figure 8C). Exposure of HSC to ethanol caused a concentration-dependent generation of acetaldehyde that was inhibited by 4-Mp, and thus depends on ADH activity (Figure 8D). S100-positive HSC in culture (Figure 8E) and in sections of human skin also expressed immunoreactive TRPA1 (Figure 8F and Supplementary Figure 2B). Cultured HSC expressed TRPA1 mRNA (Figure 8G). Exposure of HSC to AITC, acetaldehyde or H_2O_2 elicited increases in intracellular calcium that were attenuated by A967079 (Figure 8H). Prolonged exposure of HSC to ethanol induced a delayed and sustained increase in calcium responses, which was attenuated by pretreatment with 4-Mp or A967079 (Figure 8I). S100-positive HSC in culture and in sections of human skin also expressed immunoreactive NOX1 (Figure 8J and K and Supplementary Figure 2B). In addition, cultured HSC expressed NOX1 mRNA (Figure 8L). AITC, acetaldehyde or H_2O_2 elicited calcium dependent increases in H_2O_2 in HSC that were reduced by A967079 (Figure 8M).

Discussion

Our results show that intraplantar injection of ethanol in the mouse hind paw causes two sensory responses, which are temporally and mechanistically distinct. After an

immediate and short-lived (5 min) nociceptive response, mice exhibited a delayed and prolonged (1-6 h) mechanical allodynia. TRPV1 antagonism or deletion prevented the immediate nociceptive response, which is thus mediated by ethanol activation of TRPV1, as previously reported (16). In contrast, TRPV1 disruption did not affect the delayed and sustained mechanical allodynia, which occurs by a different mechanism.

Genetic or pharmacological impairment of ADH that results in increased acetaldehyde levels enhances the susceptibility of affected individuals to alcohol-evoked symptoms (13, 14). Our observation that pretreatment with the ADH inhibitor, 4-Mp, prevented the allodynia evoked by intraplantar ethanol and that intraplantar injection of acetaldehyde caused allodynia similar to that evoked by ethanol support the hypothesis that acetaldehyde mediates the prolonged allodynic effect of ethanol. The findings that genetic deletion or pharmacological antagonism of TRPA1 prevented ethanol- and acetaldehyde-evoked allodynia are consistent with the hypothesis that the aldehyde and not its precursor gates TRPA1 (20) and plays a major role in the allodynia that mimics the neuropathic pain observed in alcoholics. In contrast, deletion of TRPV4, a proalgesic channel expressed by a subset of nociceptors, did not affect either acute nociception or allodynia. Thus, while acute nociception is due to a direct action of ethanol on TRPV1, delayed and sustained allodynia is mediated by TRPA1, *via* ADH-dependent generation of acetaldehyde.

We investigated the contribution of TRPA1 to pain after oral administration of ethanol, which more closely resembles the situation in alcoholics. In contrast to intraplantar administration, intragastric administration of ethanol did not cause acute pain-related behavior. However, intragastric ethanol did cause delayed and sustained allodynia in wild-type but not *Trpa1*$^{-/-}$ mice; deletion of either TRPV1 or TRPV4 did not affect allodynia. The ability of intraperitoneal acetaldehyde to mimic the response evoked by intragastric ethanol implicates this metabolite as a mediator of TRPA1-dependent

allodynia. Although the major site of alcohol metabolism is the liver, where the bulk of acetaldehyde is generated (25, 26), several extrahepatic cells express ADH (23, 24). The ADH inhibitor, 4-Mp, when given locally (intraplantar administration), prevented acetaldehyde increase and allodynia evoked by local (intraplantar) ethanol, and, although partially, reduced increases in acetaldehyde and allodynia elicited by intragastric ethanol. Complete inhibition of allodynia and increases in acetaldehyde levels evoked by intragastric ethanol were, however, obtained by systemic 4-Mp administration. These results suggest that acetaldehyde, which mediates allodynia, derives in part from the systemic circulation, and in part from local production within the paw tissue. ADH mRNA and protein were confined to Schwann cells that ensheath sensory nerve fibers in the paw. The ability of the paw tissue and cultured mouse Schwann cells to convert ethanol into acetaldehyde in a 4-Mp-sensitive manner supports the proposal that Schwann cells are the local source of acetaldehyde, which engages TRPA1 to mediate allodynia.

Whereas the TRPA1 antagonist, A967079, inhibited ethanol-evoked allodynia when administered before or after ethanol, the ADH inhibitor, 4-Mp, prevented allodynia only when given before ethanol. This finding suggests that, whereas TRPA1 engagement is constantly required, acetaldehyde is necessary to initiate, but is not sufficient to maintain, allodynia. The transient (1-h duration) increase in acetaldehyde levels in the paw, compared to the sustained allodynia (6 h), strengthens the view that the prolonged allodynia is not maintained by acetaldehyde. Acetaldehyde can generate ROS (27, 29), which are among the several endogenous ligands of TRPA1 (17-19). H_2O_2 levels peaked in paw homogenates 1-3 h and returned to baseline 6 h after ethanol. However, in the mouse paw immunostaining for the carbonylic byproduct of oxidative stress, 4-HNE (33), a known TRPA1 activator (21), increased 3 h, and peaked 6 h after ethanol when allodynia was still robustly present. In agreement with the time courses of H_2O_2 and 4-HNE levels in the mouse paw, treatment with the ROS scavenger, PBN, attenuated

allodynia 3 h, but not 6 h, after ethanol, while the aldehyde scavenger, NAC, was effective 6 h after ethanol. These findings suggest that TRPA1 engagement by mediators efficiently scavenged by PBN does not outlast ~4 h after exposure to ethanol, whereas attenuation of allodynia 6 h after ethanol is provided exclusively by compounds able to scavenge aldehydic compounds, such as 4-HNE. The ability of the ROS scavenger, PBN, to attenuate paw allodynia indicates that oxidative stress sustains allodynia and raises the question of how ethanol/acetaldehyde generate ROS. We recently reported in a mouse model of sciatic nerve injury that ROS, which sustain mechanical allodynia, are produced *via* the TRPA1/NOX1 pathway in Schwann cells ensheathing sciatic nerve fibers (22). Therefore, we investigated the possibility that a similar mechanism contributes to ethanol-evoked allodynia. In support of this hypothesis, *Plp1-Cre^{ERT};Trpa1$^{fl/fl}$* mice, which selectively lack TRPA1 in Schwann cells, showed attenuated allodynia and reduced H_2O_2 levels in paw tissue. NOX1 has been reported as the major enzyme isoform responsible for the TRPA1-dependent oxidative burst in Schwann cells (22). We confirmed this finding since the selective NOX1 inhibitor, ML171 (34), attenuated ethanol-evoked allodynia.

Finally, we asked whether the TRPA1 which mediates ethanol-evoked allodynia is exclusively the channel expressed by Schwann cells, or if the neuronal channel might also contribute. Mice with selective deletion of TRPA1 in primary sensory neurons, *Adv-Cre;Trpa1$^{fl/fl}$* mice (31), exhibited a markedly attenuated ethanol-evoked paw allodynia. However, the increased levels of H_2O_2 in the paw tissue were unaffected. These observations indicate that the Schwann cell TRPA1/NOX1 pathway is necessary to maintain the prolonged oxidative stress generation required to target the neuronal TRPA1, which eventually sustains allodynia. *Plp1-Cre^{ERT};Trpa1$^{fl/fl}$* mice are selectively deficient of TRPA1 in the Schwann cell and oligodendrocyte lineage. Thus, the implication of oligodendrocytes in the brain signaling of allodynia evoked by intragastric

ethanol should be considered. However, several observations suggest that initiation and maintenance of paw allodynia is promoted by a series of local events driven by TRPA1 of Schwann cell ensheathing plantar nerve. *Plp1-Cre^{ERT};Trpa1$^{fl/fl}$* mice not only failed to produce allodynia, but were unable to generate the local oxidative stress response that is required to sustain allodynia. Local treatment with a TRPA1 AS-ODN or with the active tamoxifen metabolite, 4-OHT, which directly binds to the tamoxifen-inducible estrogen receptor, attenuated intragastric ethanol-evoked allodynia only in the treated paw, without affecting the pain response in the contralateral side. These findings imply that the drugs did not diffuse to distant sites, including the brain, but maintained their action confined to the treated paw. Thus, the most parsimonious hypothesis is that Schwann cell TRPA1, by promoting local oxidative stress generation, is necessary and sufficient to sustain ethanol-evoked allodynia. Nonetheless, these observations do not exclude a contribution of oligodendrocyte TRPA1 to the central processing of the pain response. The generation of mice lacking TRPA1 solely in Schwann cells would be required to definitively determine the selective role of TRPA1 in this cell type.

Painful neuropathy is produced by chronic alcohol ingestion and is associated with peculiar pathological features, such as the loss of IENF (5). We reproduced a chronic condition in mice by feeding them an ethanol containing diet. The observation that both *Trpa1$^{-/-}$* and *Plp1-Cre^{ERT};Trpa1$^{fl/fl}$* mice did not develop allodynia indicated that TRPA1 and specifically the channel expressed by Schwann cells is necessary and sufficient to generate the painful condition. Reduced levels of either H_2O_2 or 4-HNE in the plantar nerve of *Trpa1$^{-/-}$* and *Plp1-Cre^{ERT};Trpa1$^{fl/fl}$* mice and the ability of the TRPA1 antagonist and the ROS scavenger to reverse allodynia, suggest that chronic ethanol ingestion activates a proalgesic mechanism identical to that induced by acute ethanol exposure. Thus, the oxidative stress that signals pain is generated by a sustained gating of Schwann cell TRPA1 by acetaldehyde generated by the daily ethanol ingestion.

Our results show that in mice receiving chronic ethanol administration deletion of Schwann cell TRPA1 does not ameliorate IENF loss, but does attenuate allodynia. Thus, Schwann cell TRPA1 and the ensuing oxidative stress burst are not crucial for the neuropathy and there is no stringent correspondence between IENF degeneration and neuropathic pain. After the loss of IENF, the remaining extraepithelial nerve fibers with their ensheathing Schwann cells are sufficient to elicit mechanical allodynia. Various interventions, including the immunomodulator, minocycline (35), erythropoietin (36), a poly(ADP-ribose) polymerase inhibitor (37) and a TRPA1 antagonist (38), have been reported to attenuate IENF loss and the ensuing neuropathic pain-responses. A series of differences may explain the discrepancy with our current data, including the causative agent of the neuropathy, alcohol *vs.* streptozotocin and paclitaxel, or in the case of TRPA1, systemic treatment with an antagonist that non-selectively targets TRPA1, not solely in Schwann cells, but in all cells where it is expressed.

The presence of thiamine deficiency in heavy alcohol drinkers suggested that the beriberi neuropathy was the underlying cause of the neurological symptoms in alcoholics. However, investigation of respective clinicopathological features has clearly differentiated the two conditions (7). Alcoholic neuropathy is sensory-dominant and predominantly shows loss of small fibers, while thiamine deficiency neuropathy is motor-dominant with mainly large fiber loss (7). The small-fiber polyneuropathy documented in heavy alcohol drinkers with normal thiamine status (39) further supported the direct role of alcohol and acetaldehyde, and not of thiamine deficiency, in alcoholic neuropathy (7, 39, 40). Assessment of ethanol-evoked allodynia in mice underscores the implication of TRPA1 either in acute (single administration) or chronic (prolonged exposure) settings. However, pain (with or without burning quality) is the initial major symptom of alcoholic neuropathy; it develops slowly, extending over a period of months, and is associated with allodynia and hyperalgesia (3). Thus, a limitation of the present murine study is that only

one (mechanical allodynia) among the various pain modalities reported by alcoholics has been investigated.

While TRPV1 is key to evoke the acute nociceptive behavior caused by local exposure to ethanol, TRPA1 uniquely mediates the prolonged paw allodynia that models in mice one pain symptom observed in patients. However, multiple ethanol-derived mediators contribute to the TRPA1-mediated paw allodynia. Acetaldehyde generated by liver ADH (Supplementary Figure 6) and locally by Schwann cell ADH commits Schwann cell TRPA1/NOX1 to generate ROS. ROS released from Schwann cells engage TRPA1 in nociceptors initially and up to 3 h after ethanol. The peroxidation-dependent generation of carbonylic byproducts, including 4-HNE, sustains the final TRPA1 targeting. The translational value of the present findings is strengthened by the observation that human Schwann cells are fully equipped to exert all the functions found in mouse Schwann cells. Human Schwann cells express ADH, TRPA1 and NOX1 mRNA and protein, and are capable of converting ethanol into acetaldehyde. Human Schwann cells respond to ethanol (*via* acetaldehyde), acetaldehyde and H_2O_2 with a TRPA1-dependent calcium response and the ensuing generation of oxidative stress. Thus, inhibition of any of the steps reported here in mice may be translated to human Schwann cells and could be beneficial to attenuate pain associated with alcohol consumption in patients.

The presence of ADH in Schwann cells that express TRPA1/NOX1 and their ability of generating oxidative stress identifies an autocrine pathway that we propose as a major contributing mechanism in alcohol-induced mechanical allodynia. Moreover, this pathway may be important in other conditions produced by exposure to alcohol. The reported presence of TRPA1 in oligodendrocytes (41) suggests that similar detrimental mechanisms may operate in the central nervous system to mediate the toxic effect

associated with alcohol ingestion. Further studies are required to explore whether Schwann cell TRPA1 mediates pain-like responses evoked by chronic ethanol in humans.

Methods

Animals

The following mouse strains were used: C57BL/6J (male, 20-25 g, 5-6 wk; Envigo); littermate WT (*Trpa1*$^{+/+}$) and TRPA1-deficient mice (*Trpa1*$^{-/-}$, B6.129P-Trpa1^{tm1Kykw}/J, 25-30 g, 5-8 wk, Jackson Laboratories) (42); littermate WT (*Trpv4*$^{+/+}$) and TRPV4-deficient (*Trpv4*$^{-/-}$) mice (25-30 g, 5-8 wk) (43); and littermate WT (*Trpv1*$^{+/+}$) and TRPV1-deficient mice (*Trpv1*$^{-/-}$, B6.129X1-Trpv1^{tm1Jul}/J, 25-30 g, 5-8 wk, Jackson Laboratories). All these strains were generated by C57BL/6 background.

To selectively delete *Trpa1* gene in primary sensory neurons, 129S-Trpa1^{tm2Kykw}/J mice (*floxed Trpa1, Trpa1*$^{fl/fl}$, Stock No: 008649; Jackson Laboratories), which possess loxP sites on either side of the S5/S6 transmembrane domains of the *Trpa1* gene, were crossed with hemizygous *Advillin-Cre* male mice (44). The progeny (*Adv-Cre*;*Trpa1*$^{fl/fl}$) was genotyped by standard PCR for *Trpa1* and *Advillin-Cre*. Mice negative for *Advillin-Cre* (*Adv-Cre*$^{-}$;*Trpa1*$^{fl/fl}$) were used as control. Successful *Advillin-Cre* driven deletion of TRPA1 mRNA was confirmed by RT-qPCR (45). To generate mice in which the *Trpa1* gene was conditionally silenced in Schwann cells/oligodendrocytes homozygous 129S-Trpa1^{tm2Kykw}/J (*floxed TRPA1, Trpa1*$^{fl/fl}$, Stock No: 008649, Jackson Laboratories), were crossed with hemizygous B6.Cg-Tg(Plp1-Cre^{ERT})3Pop/J mice (*Plp1-Cre*^{ERT}, Stock No: 005975, Jackson Laboratories), expressing a tamoxifen-inducible Cre in myelinating cells (Plp1, proteolipid protein myelin 1) (22). The progeny (*Plp1-Cre*;*Trpa1*$^{fl/fl}$) was genotyped by standard PCR for *Trpa1* and *Plp1-Cre*^{ERT} (22). Mice negative for *Plp1-Cre*^{ERT} (*Plp1-Cre*$^{-}$;*Trpa1*$^{fl/fl}$) were used as control. Both positive and negative mice to *Cre*^{ERT} and homozygous for floxed *Trpa1* (*Plp1-Cre*^{ERT}*;Trpa1*$^{fl/fl}$ and *Plp1-Cre*$^{ERT-}$

;Trpa1$^{fl/fl}$, respectively) were treated with intraperitoneal (i.p.) tamoxifen (1 mg/100 µl in corn oil, once a day, for 5 consecutive d) (22), resulting in Cre-mediated ablation of *Trpa1* in PLP-expressing Schwann cells/oligodendrocytes. Successful Cre-driven deletion of TRPA1 mRNA was confirmed by RT-qPCR (22). In addition, some *Plp1-Cre*^{ERT}*;Trpa1*$^{fl/fl}$ and *Plp1-Cre*$^{ERT-}$*;Trpa1*$^{fl/fl}$ were treated with the activated form of tamoxifen (4-hydroxytamoxifen, 4-OHT, intraplantar, i.pl., 0.02 mg/10 µl once a day for 4 consecutive d).

Study design

Group size of n=8 animals for behavioral experiments were determined by sample size estimation using G*Power (v3.1) (46) to detect size effect in a post-hoc test with type 1 and 2 error rates of 5 and 20%, respectively. Allocation concealment of mice to vehicle(s) or treatment(s) group was performed using a randomization procedure (http://www.randomizer.org/). The assessors were blinded to the identity (genetic background or allocation to treatment group) of the animals. Identity of the animals was unmasked to assessors only after data collection. Every effort has been made to minimize the discomfort and pain of the animals in each phase of the study. Mice were housed in a temperature- and humidity-controlled *vivarium* (12 h dark/light cycle, free access to food and water, 8 animals per cage). Mice were acclimatized in a quiet, temperature-controlled room (20-22°C) for 1 h before behavioral studies, that were done between 9 a.m. and 5 p.m. Animals were anaesthetized with a mixture of ketamine and xylazine (90 mg/kg and 3 mg/kg, respectively, i.p.) and euthanized with inhaled CO_2 plus 10-50% O_2. If not otherwise indicated, reagents were obtained from Sigma-Aldrich (Milan, Italy).

In functional and biochemical studies ethanol was given by i.pl. (30%) or i.g. (15%, 4 ml/kg) administration and acetaldehyde by i.pl. (20 nmol) or i.p. (0.1 mg/kg) administration. Vehicle of i.pl. or i.g. ethanol and i.pl. or i.p. acetaldehyde was 0.9%

NaCl. Vehicle the various drugs was 4% DMSO and 4% Tween80 in 0.9% NaCl for i.pl. or i.p. administration and, 0.5% carboxymethylcellulose for i.g. administration. Twenty µl/site were injected in all i.pl. administrations. SB366791, N-(3-methoxyphenyl)-4-chlorocinnamide (1 mg/kg, i.p.) or vehicle were administered 30 min before i.pl. ethanol or vehicle. A967079, [(1E,3E)-1-(4-Fluorophenyl)-2-methyl-1-penten-3-one oxime] and phenyl-α-tert-butyl nitrone (PBN) (both, 100 mg/kg, i.p. or 100 µg i.pl.) or their vehicle, were administered 1 h after i.pl. or i.g. ethanol and i.pl. or i.p. acetaldehyde or their vehicle. PBN (100 mg/kg, i.p.) or vehicle were also given 5 h after i.g. ethanol. 4-methylpyrazole (4-Mp, 50 mg/kg, i.g. or 100 µg, i.pl.) or vehicle were administered 30 min before i.pl. or i.g. ethanol or vehicle and 2 h after i.g. ethanol or vehicle. N-acetyl cysteine (NAC, 250 mg/kg, i.p.) or vehicle were administered 5 h after i.g. ethanol. ML171 [2-acetylphenothiazine] (60 mg/kg, i.p.) (Tocris Bioscience) or vehicle were administered 2 h after i.g. ethanol and i.p. acetaldehyde or their vehicles.

Phosphorothioate-modified TRPA1 AS-ODN (sequence: 5'-TATCGCTCCACATTGCTAC-3') and TRPA1 MM-ODN (sequence: 5'-ATTCGCCTCACATTGTCAC-3') (22) (10 nmol/10 µl, i.pl.) were administered once a day for 4 consecutive d. Some mice treated with TRPA1 AS/MM-ODN or with 4-OHT were tested for the acute nociceptive response to AITC (20 nmol, i.pl.) or ethanol (30%, i.pl.) or their vehicles (0.5% DMSO or 0.9% NaCl, respectively).

Blood for ethanol assay was obtained from anesthetized mice at 15, 30, 60 and 180 min after i.g. ethanol. Liver and hind paw tissues for ethanol and acetaldehyde assays were obtained from mice euthanized 15, 30, 60 and 180 min after i.pl. or i.g. ethanol. Some mice were treated with 4-Mp (100 µg, i.pl. or 50 mg/kg, i.g.) 30 min before or 1 hr after i.pl. or i.g. ethanol or their vehicles and euthanized 2 h after ethanol. For H_2O_2 assay, hind paw tissues were taken from mice euthanized before and 1, 3, 6 and 8 h after i.pl. or i.g. ethanol and acetaldehyde or their vehicles. In additional experiments, paw

tissues were taken from mice treated 3 h before with i.pl. or i.g. ethanol or acetaldehyde or their vehicles that 1 h before with A967079 (100 mg/kg, i.p.) or PBN (100 mg/kg, i.p.) or their vehicles. For the 4-HNE-histidine protein adducts assay, paw tissues were taken from mice euthanized before and 1, 3, 6 and 8 h after i.g. ethanol.

For chronic alcohol administration, one or two mice were housed *per* cage and were initially fed the control Lieber-DeCarli diet (F1259, Bio-Serv) *ad libitum* for 5 d to acclimatize them to the liquid food and tube feeding. Afterward, ethanol-fed groups were allowed free access to the ethanol Lieber-DeCarli diet containing 5% (vol/vol) ethanol (F1258, Bio-Serv), daily for 28 d (32). Control mice were pair-fed (*i.e.* calorically matched to the ethanol-fed mice) with the control diet in which equal calories of maltose-dextrin was consumed in place of ethanol (32). The feeding tubes contained 30 or 50 ml of ethanol or control liquid diet for one or two mice, respectively. Mice in both the experimental groups were healthy and, displayed normal reflexes and alertness. A967079 and PBN (both, 100 mg/kg, i.p.), were administered at day 28 after ethanol or control liquid diet. Liver and paw tissues for ethanol and acetaldehyde assays were obtained from mice euthanized at day 28 after ethanol or control liquid diet.

Acute nociceptive behavior, hind paw mechanical allodynia and rotarod test

To assess acute nociceptive responses, mice were placed in a plexiglass chamber immediately after ethanol (15-80% in 0.9% NaCl, i.pl.), acetaldehyde (0.1-10 nmol/site in NaCl, i.pl.), allyl isothiocyanate (AITC, 10 nmol in 0.5% DMSO, i.pl.) or their respective vehicles, and the total time (nociception time, s) spent in licking and lifting the injected right hind limb (21) was recorded for 5 min. Mechanical allodynia was evaluated by applying the von Frey filaments to the posterior hind paw of mice, before (basal threshold) and after (1-24 h) ethanol (15-80% in 0.9% NaCl, i.pl.; 1-4 ml/kg of 15% in 0.9% NaCl, i.g.), acetaldehyde (1-20 nmol/site in 0.9% NaCl, i.pl.; 0.1-1 mg/kg in 0.9%

NaCl, i.p.) or respective vehicles and, in mice fed with the Lieber-DeCarli or control diet over 28 d. Mechanical threshold was determined by using the up-and-down paradigm (47).

Locomotor function, coordination, and sedation of animals were tested by using a rotarod apparatus (UgoBasile). Twenty-four h before the experiments, mice were trained on the rotarod apparatus, programmed at 8 rpm, until they remained without falling for 60 s. The day of the experiment, the latency (s) to the first fall and the number of falls were recorded. Cut-off time was 240 s.

Ethanol, acetaldehyde, H_2O_2 and 4-HNE-histidine protein adducts assays

For ethanol assay, blood taken into heparin containing syringes *via* direct cardiac puncture from anesthetized mice, was centrifuged at 10,000 rpm for 5 min and the plasma was collected. For ethanol and acetaldehyde assay paw and liver tissues from euthanized mice were homogenized in PBS (0.1 M) by using a tissue homogenizer (Qiagen SpA) for 30 s, centrifuged 10,000 rpm for 10 min, and supernatants collected. Ethanol content was determined by a colorimetric assay (ab65343, Abcam) according to the manufacturer's protocol, and expressed as nmol/ml (plasma) and nmol/mg of protein (tissues). Acetaldehyde content (nmol/mg of protein) was determined by a colorimetric assay (Megazyme) according to the manufacturer's protocol.

The H_2O_2 content was determined in the paw tissue by using the Amplex Red® assay (Invitrogen). Briefly, tissues were rapidly placed into modified Krebs/HEPES buffer (composition in mmol/l: 99.01 NaCl, 4.69 KCl, 2.50 $CaCl_2$, 1.20 $MgSO_4$, 1.03 KH_2PO_4, 25.0 $NaHCO_3$, 20.0 Na-HEPES, and 5.6 glucose [pH 7.4]), minced and incubated with Amplex red (100 μM) and HRP (1 U/ml) (1 hour, 37°C) in modified Krebs/HEPES buffer protected from light (48). Fluorescence excitation and emission were at 540 and 590 nm, respectively. H_2O_2 production was calculated using H_2O_2

standard and expressed as µmol/l of mg of dry tissue.

4-HNE-histidine (4-HNE-His) protein adduct content was quantified in paw tissues by a colorimetric assay (OxiSelect HNE-His Adduct ELISA Kit, Cell Biolabs, Inc) according to manufacturer's protocol. Paw tissues were homogenized in PBS (0.1 M), added of a protease inhibitor cocktail (1 tablet/100 ml) for 30 s and centrifuged (10,000 rpm, 10 min, 4°C). Supernatants were assayed for the measurement of total protein content by a Bradford assay (Bio-Rad) and 4-HNE-His content (expressed as µg/mg of protein).

Cell cultures

Human embryonic kidney 293 (HEK293) cells stably transfected with the cDNA for human TRPA1 (hTRPA1-HEK293) were cultured as previously described (49). Human Schwann cells (HSC, #1700, CliniScience) were cultured in Schwann cell medium (#1701, CliniScience) according to the manufacturer's protocol. Human alveolar type II epithelium-like adherent cell line (A549) (CCL-185™, American Type Culture Collection) were cultured in RPMI with 10% FBS, 2 mM glutamine, 100 U penicillin, 100 µg/ml streptomycin and 1 mM HEPES. All cells were used when received without further authentication.

Schwann cells were isolated from sciatic nerves of C57BL/6J mice. The epineurium was removed, and nerve explants were divided into 1 mm segments and dissociated enzymatically using collagenase (0.05%) and hyaluronidase (0.1%) in HBSS (2 h, 37°C). Cells were collected by centrifugation (800 rpm, 10 min, room temperature) and the pellet was resuspended and cultured in DMEM containing: 10% fetal calf serum, 2 mM L-glutamine, 100 U/ml penicillin, 100 mg/ml streptomycin. Three days later, cytosine arabinoside (10 mM) was added to remove fibroblasts. All cells were cultured in an atmosphere of 95% air and 5% CO_2 at 37°C.

Assays in cultured cells

Calcium imaging. HSC were plated on glass coated (poly-L-lysine, 8.3 μM) coverslips and $[Ca^{2+}]_i$ response was measured as previously reported (22). HSC were exposed to AITC (100 μM), H_2O_2 (10 mM) and acetaldehyde (10 mM) or their vehicles (0.1% DMSO or 0.9% NaCl) in the presence or absence of A967079 (50 μM) or its vehicle (0.3% DMSO). In other experiments, HSC were exposed to ethanol (10 mM) or its vehicle. In this case the delayed $[Ca^{2+}]_i$ response was monitored for ~150 min in the presence or absence of A967079 (50 μM) or 4-Mp (100 μM) or their vehicle (0.3% DMSO). Results were expressed as % increase in $Ratio_{340/380}$ over baseline normalized to the maximum effect induced by ionomycin (5 μM) added at the end of each experiment.

Acetaldehyde assay. Mouse Schwann cells and HSC were plated in 48-well plates in 5% CO_2 and 95% O_2 at 37°C until 90% of confluence. The cultured medium was replaced with PBS added with ethanol (1-100 mM), ethanol (10 mM) plus 4-Mp (100 μM) or vehicle (0.9% NaCl) and maintained in 5% CO_2 and 95% O_2 at 37°C for 3 h. Then, supernatants were collected, and acetaldehyde content was assayed by using a colorimetric assay (Megazyme) according to the manufacturer's protocol. Acetaldehyde content was expressed as μmol/l. The cytotoxicity to different stimuli was tested by using the MTT assay viability test.

H_2O_2 assay. H_2O_2 was determined by the Amplex Red® assay. HSC were plated in 96-well clear bottom black ($5x10^5$ cells/well) and maintained in 5% CO_2/95% O_2 (24 h, 37°C). The cultured medium was replaced with Krebs/HEPES added with A967079 (30 μM) or vehicle (0.3% DMSO) for 10 min at room temperature. HSC were stimulated with AITC (100 μM), H_2O_2 (200 nM) and acetaldehyde (10 mM) or their vehicle (0.01% DMSO, Krebs/HEPES), added with Amplex red (50 μM) and HRP (1 U/ml, 30 min, room temperature, protected from light). Some experiments were performed in Ca^{2+}-free

Krebs/HEPES buffer containing ethylenediaminetetraacetic acid (EDTA, 1 mM). Signal was detected 60 min after exposure to stimuli. H_2O_2 release was calculated using H_2O_2 standards and expressed as nmol/l.

Immunofluorescence

Anesthetized mice were transcardially perfused with PBS and 4% paraformaldehyde. Paw tissues were removed, post-fixed for 24 h, and paraffin embedded. Human and mouse FFPE sections (5 μm) were incubated with primary antibodies (all from Abcam): TRPA1 (ab58844, rabbit polyclonal, 1:400), S100 (ab14849, mouse monoclonal [4B3], 1:300), protein gene product 9.5 (PGP9.5, ab8189, mouse monoclonal [13C4/I3C4], 1:600), NOX1 (ab131088, rabbit polyclonal, 1:250), 4-HNE (HNEJ-2, ab48506, mouse monoclonal, 1:40) and alcohol dehydrogenase (ab108203, rabbit monoclonal [EPR4439], 1:200) diluted in fresh blocking solution (PBS, pH 7.4, 2.5% NGS). To confirm specificity, TRPA1, NOX1 and ADH primary antibodies were pre-adsorbed (1:1, overnight, 4°C, before adding to tissue sections) with their respective antigen peptides: TRPA1 synthetic peptide (sequence: CEKQHELIKLIIQKME, Twin Helix srl); ADH recombinant protein, (#NBP1-99053, Novus Biologicals), NOX1 recombinant protein (#PCPKAB7187921P, Promocell). Sections were then incubated with the fluorescent polyclonal secondary antibodies, Alexa Fluor 488 and 594 (1:600, Invitrogen), and coverslipped using mounting medium with DAPI (Abcam). The product of the differences from the mean (PDM) image was used for the qualitative analysis of colocalization. The PDM image is a pseudo-colored, generated by pixel that is equal to the PDM value at the location (Image J, NIH).

Human Schwann cells were grown on glass coated (poly-L-lysine, 8.3 μM) coverslips and cultured for 2-3 days before staining. Cells were fixed in ice-cold methanol/acetone (5 min at -20°C), washed with PBS and blocked with NGS (10%) (1 h,

room temperature). The cells were incubated with primary antibodies: TRPA1 (ab58844, rabbit polyclonal, 1:400), S100 (ab14849, mouse monoclonal [4B3], 1:300), NOX1 (ab131088, rabbit polyclonal, 1:250) and alcohol dehydrogenase (ab108203, rabbit monoclonal [EPR4439], 1:200) diluted in fresh blocking solution (PBS, pH 7.4, 2.5% NGS). Cells were finally incubated with fluorescent polyclonal secondary antibodies (1:600, Alexa Fluor 488, and 594, Invitrogen) (2 h, room temperature) and mounted using mounting medium with DAPI (Abcam). Fluorescence images were obtained using an BX51 microscope (Olympus).

Immunohistochemistry and intraepidermal nerve fiber (IENF) analysis

Anesthetized mice were transcardially perfused with PBS and 4% paraformaldehyde. Mice paws were placed overnight at 4°C in 10% formalin, transferred to 30% sucrose overnight and frozen and cryosectioned at 30 µm transversal to long paw axis. Free floating sections were incubated in PBS containing 0.1% Triton X-100 (TBS) and 2.5% NGS 1 hour at room temperature, then in the primary antibody panaxonal marker PGP9.5 (ab108986, rabbit monoclonal [EPR4118] 1:600, Abcam) overnight at room temperature. Afterward, sections were rinsed in TBS and placed in secondary biotinylated goat anti-rabbit IgG antibody (Vector Laboratories), 1:300, 2 hour at room temperature, placed in avidin-biotin complex solution (Vectastain Elite ABC HRP, Vector Laboratories) for 30 min at room temperature, followed by rinsing in TBS. The sections were then transferred into ImmPACT DAB (Vector Laboratories) to 4-6 min for the chromogen development reaction and rinsed in distilled water before mounting. IENF were counted either under microscope at 40X magnification. Single PGP9.5-positive fibers crossing the epidermis-dermis boundary (basal membrane) were counted. Secondary branching is excluded from quantification, according to the European Federation of Neurological Societies guidelines (50).

Real-Time PCR

RNA was extracted from paw tissue and liver obtained from C57BL/6J mice or from human Schwann cells. Total RNA was extracted using the RNeasy Mini kit (Qiagen SpA), according to the manufacturer's protocol. RNA concentration and purity were assessed spectrophotometrically. Reverse transcription was performed with the Qiagen QuantiTect Reverse Transcription Kit (Qiagen SpA) following the manufacturer's protocol. For mRNA relative quantification, rt-PCR was performed on Rotor Gene® Q (Qiagen SpA). The sets of probes for human cells were: ACTB (β-actin): Primer1 CCT TGC ACA TGC CGG AG Primer2 ACA GAG CCT CGC CTT TG Probe /56-FAM/TCA TCC ATG /ZEN/GTG AGC TGG CGG /3IABkFQ/ (NCBI Ref Seq: NM_001101); TRPA1: Primer1 GAA ACC AAA GTG GCA GCT TC Primer2 GAC ATT GCT GAG GTC CAG AA Probe /56-FAM/TGA AGT TCC /ZEN/ACC TGC ATA GCT ATC CTC T/3IABkFQ/ (NCBI Ref Seq: NM_007332); NOX1 Primer1 AAA CAT TCA GCC CTA ACC AAA C Primer2 GAA TCT TCC CTG TTG CCT AGA Probe /56-FAM/ACC ACC CAG /ZEN/TTT CCC ATT GTC AAG A/3IABkFQ/ (NCBI Ref Seq:NM013955); ADH1A: Primer1 GTT TCT TTA ACT CCC ATA GCA CAG Primer2 CAC AAG GAC TCA CCA GTC TC Probe /56-FAM/AGA CAG AAT /ZEN/CAA CAT GAG CAC AGC AGG /3IABkFQ/ (NCBI Ref Seq: NM_000667); ADH1B: Primer1 GTG CTC ATG TCG TTT CTG TCT Primer2 TCA AGC AGA GAA GAA ATC CAC AA Probe/56-FAM/TGC CCA CCA /ZEN/GCA GAC TGT GA/3IABkFQ/ (NCBI Ref Seq: NM_000668), ADH1C: Primer1 ATC TTA ATG CGA ACT TCA TGA GC Primer2 CAG AAT CAA TAT GAG CAC AGC AG Probe /56-FAM/CCA TTG AGG /ZEN/AGG TAG AGG TTG CAC C/3IABkFQ/ (NCBI Ref Seq: NM_000669); ADH4: Primer1 AGA AAG ACC CAC ACC TCC TA Primer2 GAG TTT GTC TGC TTG GAT GTG Probe /56-FAM/CCC TGG TTC /ZEN/GAC TTG TGC TGT CT/3IABkFQ/ (NCBI

Ref Seq: NM_000670); ADH5: Primer1 TGC CAC CTC TAT CTC CTC TAT G Primer2 CCG ACC AGA ATC CGT GAA C Probe /56-FAM/AGC CTT GCA /ZEN/CTT GAT AAC CTC GTT CG/3IABkFQ/ (NCBI Ref Seq: NM_000671); ADH6: Primer1 TGT GGC AGA AAG AGT GTG AT Primer2 CCT CTT GTA TCC CAC CAT CTT G Probe /56-FAM/TCA CCT GGT /ZEN/TTC ACT GTG CTT ACT CC/3IABkFQ/(NCBI Ref Seq: NM_000672).

The sets of probes for mouse tissue were: ACTB: Primer1 GAC TCA TCG TAC TCC TGC TTG Primer2 GAT TAC TGC TCT GGC TCC TAG Probe /56-FAM/CTG GCC TCA /ZEN/CTG TCC ACC TTC C/3IABkFQ/ (NCBI Ref Seq: NM_001101); ADH1: Primer1 AAGACT ACAGCAAACCCATCC Primer2 GACGACGCTT ACACCACAT Probe /56-FAM/CCTTGACAC/Z EN/CA TGACTTCTGCCCT /31ABkFQ/ (NCBI Ref Seq: NM_007409); ADH5: Primer1 TCATCCCACTCT ACATCCCA Primer2 GGT AAATCTGCT AGTCCCATCT Probe /56-FAM/CCCTTCCCC/Z EN/TGAGTGACCCTT A TTTTC/31ABkFQ/ (NCBI Ref Seq NM_007410); ADH7: Primer1 TGAAGTT ATTGGGCGTCTTGA Primer2 GTCATAGGTGAGCATCTTGGC Probe /56-FAM/CAGTGTGGT /Z EN/GGTTGGTGCTCCT /31ABkFQ/ (NCBI Ref Seq NM_009626).

The chosen reference gene was the ACTB. The QuantiTect Probe PCR Kits (Qiagen SpA) was used for amplification, and the cycling conditions were: samples were heated to 95°C for 10 min followed by 40 cycles of 95°C for 15 s, and 65°C for 20 s. PCR reaction was carried out in triplicate. Relative expression of mRNA was calculated using the $2^{-\Delta(\Delta CT)}$ comparative method, with each gene normalized against ACTB gene for the same sample.

Statistical analysis

Statistical analysis was performed by the unpaired two-tailed Student's t-test for

comparisons between two groups. Group means were compared with a one-way ANOVA, followed, as needed, by the pair-wise comparison of multiple groups that employed the Bonferroni's correction to maintain the experiment-wise error rate at 5%. For behavioural experiments with repeated measures, a two-way mixed model was used to compare the control and treated groups of mice at each time point tested, using the Bonferroni's correction for multiple time points. Statistical analyses were performed on raw data using Prism 5 GraphPad software (GraphPad Software Inc.). $P<0.05$ was considered statistically significant.

Study Approval

The use of FFPE sections of human skin samples was approved by the Local Ethics Committee (#11989_bio/2018), according to the Helsinki Declaration, and informed consent was obtained. All applicable international, national, and/or institutional guidelines for the care and use of animals were followed. In vivo experiments were in accordance to European Union (EU) guidelines and Italian legislation (DLgs 26/2014, EU Directive application 2010/63/EU) for animal care procedures, and under the University of Florence research permit #194/2015-PR. Animal studies were reported in compliance with the ARRIVE guidelines (51).

Author contributions.

FDL, RP, PG and RN designing research studies; FDL, SLP, LL, FP, DSMdA and RN conducting experiments; FDL, SLP, LL, FP, DSMdA and RN acquiring data; FDL, MNJ and RN analyzing data; AI providing human tissue samples; FDL, MNJ, RP, NWB, PG and RN writing the manuscript.

Acknowledgments.

We thank AH Morice (University of Hull, UK) for hTRPA1-HEK293 cells and D. Preti (University of Ferrara, Italy) for providing A967079. We also thank Mary K. Lokken for her expert English revision. This study was funded by Ministry for University and Scientific Research (MiUR) Rome, Italy Grant PRIN 201532AHAE_003 (P.G.), and by grants from the National Institutes of Health (NS102722, DE026806, DK118971) and Department of Defense (W81XWH1810431) (N.W.B.).

References

1. Rehm J, Mathers C, Popova S, Thavorncharoensap M, Teerawattananon Y, and Patra J. Global burden of disease and injury and economic cost attributable to alcohol use and alcohol-use disorders. *Lancet.* 2009;373(9682):2223-33.
2. Organization WH. *Global status report on alcohol and health 2018.* 2018.
3. Chopra K, and Tiwari V. Alcoholic neuropathy: possible mechanisms and future treatment possibilities. *Br J Clin Pharmacol.* 2012;73(3):348-62.
4. Singleton CK, and Martin PR. Molecular mechanisms of thiamine utilization. *Curr Mol Med.* 2001;1(2):197-207.
5. Mellion M, Gilchrist JM, and de la Monte S. Alcohol-related peripheral neuropathy: nutritional, toxic, or both? *Muscle Nerve.* 2011;43(3):309-16.
6. Koike H, Misu K, Hattori N, Ito S, Ichimura M, Ito H, et al. Postgastrectomy polyneuropathy with thiamine deficiency. *J Neurol Neurosurg Psychiatry.* 2001;71(3):357-62.
7. Koike H, Iijima M, Sugiura M, Mori K, Hattori N, Ito H, et al. Alcoholic neuropathy is clinicopathologically distinct from thiamine-deficiency neuropathy. *Ann Neurol.* 2003;54(1):19-29.
8. Cederbaum AI. Alcohol metabolism. *Clin Liver Dis.* 2012;16(4):667-85.
9. Eriksson CJ. The role of acetaldehyde in the actions of alcohol (update 2000). *Alcohol Clin Exp Res.* 2001;25(5 Suppl ISBRA):15S-32S.
10. Andrici J, Hu SX, and Eslick GD. Facial flushing response to alcohol and the risk of esophageal squamous cell carcinoma: A comprehensive systematic review and meta-analysis. *Cancer Epidemiol.* 2016;40:31-8.
11. Bagnardi V, Rota M, Botteri E, Tramacere I, Islami F, Fedirko V, et al. Light alcohol drinking and cancer: a meta-analysis. *Ann Oncol.* 2013;24(2):301-8.
12. Boffetta P, and Hashibe M. Alcohol and cancer. *Lancet Oncol.* 2006;7(2):149-56.

13. Xiao Q, Weiner H, and Crabb DW. The mutation in the mitochondrial aldehyde dehydrogenase (ALDH2) gene responsible for alcohol-induced flushing increases turnover of the enzyme tetramers in a dominant fashion. *J Clin Invest.* 1996;98(9):2027-32.

14. Wall TL, Peterson CM, Peterson KP, Johnson ML, Thomasson HR, Cole M, et al. Alcohol metabolism in Asian-American men with genetic polymorphisms of aldehyde dehydrogenase. *Ann Intern Med.* 1997;127(5):376-9.

15. Chen CH, Ferreira JC, Gross ER, and Mochly-Rosen D. Targeting aldehyde dehydrogenase 2: new therapeutic opportunities. *Physiol Rev.* 2014;94(1):1-34.

16. Trevisani M, Smart D, Gunthorpe MJ, Tognetto M, Barbieri M, Campi B, et al. Ethanol elicits and potentiates nociceptor responses via the vanilloid receptor-1. *Nat Neurosci.* 2002;5(6):546-51.

17. Andersson DA, Gentry C, Moss S, and Bevan S. Transient receptor potential A1 is a sensory receptor for multiple products of oxidative stress. *J Neurosci.* 2008;28(10):2485-94.

18. Takahashi N, Kuwaki T, Kiyonaka S, Numata T, Kozai D, Mizuno Y, et al. TRPA1 underlies a sensing mechanism for O2. *Nat Chem Biol.* 2011;7(10):701-11.

19. Nassini R, Materazzi S, Benemei S, and Geppetti P. The TRPA1 channel in inflammatory and neuropathic pain and migraine. *Rev Physiol Biochem Pharmacol.* 2014;167:1-43.

20. Bang S, Kim KY, Yoo S, Kim YG, and Hwang SW. Transient receptor potential A1 mediates acetaldehyde-evoked pain sensation. *Eur J Neurosci.* 2007;26(9):2516-23.

21. Trevisani M, Siemens J, Materazzi S, Bautista DM, Nassini R, Campi B, et al. 4-Hydroxynonenal, an endogenous aldehyde, causes pain and neurogenic

inflammation through activation of the irritant receptor TRPA1. *Proc Natl Acad Sci U S A.* 2007;104(33):13519-24.

22. De Logu F, Nassini R, Materazzi S, Carvalho Goncalves M, Nosi D, Rossi Degl'Innocenti D, et al. Schwann cell TRPA1 mediates neuroinflammation that sustains macrophage-dependent neuropathic pain in mice. *Nat Commun.* 2017;8(1):1887.
23. Galter D, Carmine A, Buervenich S, Duester G, and Olson L. Distribution of class I, III and IV alcohol dehydrogenase mRNAs in the adult rat, mouse and human brain. *Eur J Biochem.* 2003;270(6):1316-26.
24. Zgombic-Knight M, Ang HL, Foglio MH, and Duester G. Cloning of the mouse class IV alcohol dehydrogenase (retinol dehydrogenase) cDNA and tissue-specific expression patterns of the murine ADH gene family. *J Biol Chem.* 1995;270(18):10868-77.
25. Seitz HK, and Meier P. The role of acetaldehyde in upper digestive tract cancer in alcoholics. *Transl Res.* 2007;149(6):293-7.
26. Zakhari S. Overview: how is alcohol metabolized by the body? *Alcohol Res Health.* 2006;29(4):245-54.
27. Szuster-Ciesielska A, Plewka K, Daniluk J, and Kandefer-Szerszen M. Zinc supplementation attenuates ethanol- and acetaldehyde-induced liver stellate cell activation by inhibiting reactive oxygen species (ROS) production and by influencing intracellular signaling. *Biochem Pharmacol.* 2009;78(3):301-14.
28. Hoyt LR, Randall MJ, Ather JL, DePuccio DP, Landry CC, Qian X, et al. Mitochondrial ROS induced by chronic ethanol exposure promote hyper-activation of the NLRP3 inflammasome. *Redox Biol.* 2017;12:883-96.

29. Vrsalovic M, Vrsalovic MM, Presecki AV, and Lukac J. Modulating role of alcohol and acetaldehyde on neutrophil and monocyte functions in vitro. *J Cardiovasc Pharmacol.* 2007;50(4):462-5.

30. Aldini G, Carini M, Yeum KJ, and Vistoli G. Novel molecular approaches for improving enzymatic and nonenzymatic detoxification of 4-hydroxynonenal: toward the discovery of a novel class of bioactive compounds. *Free Radic Biol Med.* 2014;69:145-56.

31. Marone IM, De Logu F, Nassini R, De Carvalho Goncalves M, Benemei S, Ferreira J, et al. TRPA1/NOX in the soma of trigeminal ganglion neurons mediates migraine-related pain of glyceryl trinitrate in mice. *Brain.* 2018;6(5050181).

32. Bertola A, Mathews S, Ki SH, Wang H, and Gao B. Mouse model of chronic and binge ethanol feeding (the NIAAA model). *Nat Protoc.* 2013;8(3):627-37.

33. Dalle-Donne I, Aldini G, Carini M, Colombo R, Rossi R, and Milzani A. Protein carbonylation, cellular dysfunction, and disease progression. *J Cell Mol Med.* 2006;10(2):389-406.

34. Gianni D, Taulet N, Zhang H, DerMardirossian C, Kister J, Martinez L, et al. A novel and specific NADPH oxidase-1 (Nox1) small-molecule inhibitor blocks the formation of functional invadopodia in human colon cancer cells. *ACS Chem Biol.* 2010;5(10):981-93.

35. Boyette-Davis J, and Dougherty PM. Protection against oxaliplatin-induced mechanical hyperalgesia and intraepidermal nerve fiber loss by minocycline. *Exp Neurol.* 2011;229(2):353-7.

36. Bianchi R, Buyukakilli B, Brines M, Savino C, Cavaletti G, Oggioni N, et al. Erythropoietin both protects from and reverses experimental diabetic neuropathy. *Proc Natl Acad Sci U S A.* 2004;101(3):823-8.

37. Obrosova IG, Xu W, Lyzogubov VV, Ilnytska O, Mashtalir N, Vareniuk I, et al. PARP inhibition or gene deficiency counteracts intraepidermal nerve fiber loss and neuropathic pain in advanced diabetic neuropathy. *Free Radic Biol Med.* 2008;44(6):972-81.

38. Koivisto A, Hukkanen M, Saarnilehto M, Chapman H, Kuokkanen K, Wei H, et al. Inhibiting TRPA1 ion channel reduces loss of cutaneous nerve fiber function in diabetic animals: sustained activation of the TRPA1 channel contributes to the pathogenesis of peripheral diabetic neuropathy. *Pharmacol Res.* 2012;65(1):149-58.

39. Mellion ML, Silbermann E, Gilchrist JM, Machan JT, Leggio L, and de la Monte S. Small-fiber degeneration in alcohol-related peripheral neuropathy. *Alcohol Clin Exp Res.* 2014;38(7):1965-72.

40. Zambelis T, Karandreas N, Tzavellas E, Kokotis P, and Liappas J. Large and small fiber neuropathy in chronic alcohol-dependent subjects. *J Peripher Nerv Syst.* 2005;10(4):375-81.

41. Hamilton, K K, E K, and Attwell. Proton-gated Ca(2+)-permeable TRP channels damage myelin in conditions mimicking. *D - 0410462.* 2016;529(7587):523-7.

42. Kwan KY, Allchorne AJ, Vollrath MA, Christensen AP, Zhang DS, Woolf CJ, et al. TRPA1 contributes to cold, mechanical, and chemical nociception but is not essential for hair-cell transduction. *Neuron.* 2006;50(2):277-89.

43. Liedtke W, and Friedman JM. Abnormal osmotic regulation in trpv4(-/-) mice. *Proceedings of the National Academy of Sciences of the United States of America.* 2003;100(23):13698-703.

44. Guan Z, Kuhn JA, Wang X, Colquitt B, Solorzano C, Vaman S, et al. Injured sensory neuron-derived CSF1 induces microglial proliferation and DAP12-dependent pain. *Nat Neurosci.* 2016;19(1):94-101.

45. Zappia KJ, O'Hara CL, Moehring F, Kwan KY, and Stucky CL. Sensory Neuron-Specific Deletion of TRPA1 Results in Mechanical Cutaneous Sensory Deficits. *eNeuro.* 2017;4(1):0069-16.

46. Faul F, Erdfelder E, Buchner A, and Lang AG. Statistical power analyses using G*Power 3.1: tests for correlation and regression analyses. *Behav Res Methods.* 2009;41(4):1149-60.

47. Dixon WJ. Efficient analysis of experimental observations. *Annu Rev Pharmacol Toxicol.* 1980;20:441-62.

48. Landmesser U, Dikalov S, Price SR, McCann L, Fukai T, Holland SM, et al. Oxidation of tetrahydrobiopterin leads to uncoupling of endothelial cell nitric oxide synthase in hypertension. *J Clin Invest.* 2003;111(8):1201-9.

49. Sadofsky LR, Sreekrishna KT, Lin Y, Schinaman R, Gorka K, Mantri Y, et al. Unique Responses are Observed in Transient Receptor Potential Ankyrin 1 and Vanilloid 1 (TRPA1 and TRPV1) Co-Expressing Cells. *Cells.* 2014;3(2):616-26.

50. Lauria G, Hsieh ST, Johansson O, Kennedy WR, Leger JM, Mellgren SI, et al. European Federation of Neurological Societies/Peripheral Nerve Society Guideline on the use of skin biopsy in the diagnosis of small fiber neuropathy. Report of a joint task force of the European Federation of Neurological Societies and the Peripheral Nerve Society. *Eur J Neurol.* 2010;17(7):903-12, e44-9.

51. Kilkenny C, Browne WJ, Cuthill IC, Emerson M, and Altman DG. Improving bioscience research reporting: The ARRIVE guidelines for reporting animal research. *J Pharmacol Pharmacother.* 2010;1(2):94-9.

Figures

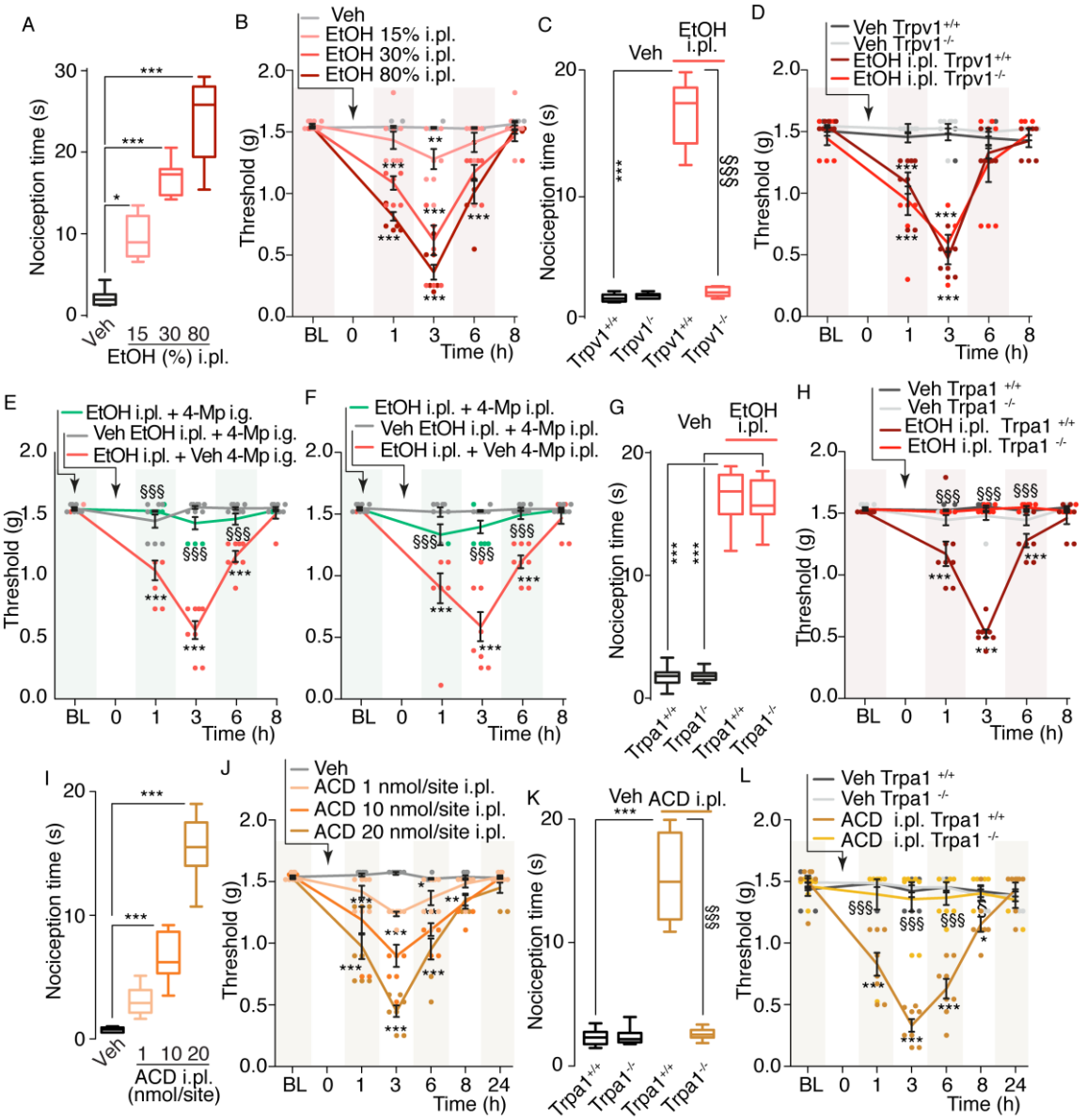

Figure 1. TRPV1 mediates acute nociception and TRPA1 mediates allodynia evoked by local ethanol. (**A**) Dose-dependent acute nociception and (**B**) dose- and time-dependent mechanical allodynia evoked by intraplantar (i.pl., 20 µl) ethanol (EtOH) or vehicle (Veh) in C57BL/6J mice. (**C**) Acute nociceptive response evoked by EtOH (30%, i.pl.) or Veh in *Trpv1*$^{+/+}$ and *Trpv1*$^{-/-}$ mice. (**D**) Time-dependent mechanical allodynia evoked by EtOH (30%, i.pl.) or Veh in *Trpv1*$^{+/+}$ and *Trpv1*$^{-/-}$ mice. (**E** and **F**) Time-dependent mechanical allodynia evoked by EtOH (30%, i.pl.) or Veh in C57BL/6J mice

pretreated with 4-methylpyrazole (4-Mp, 50 mg/kg, intragastric, i.g., or 100 µg, i.pl.) or Veh 4-Mp. (**G**) Acute nociceptive response and (**H**) time-dependent mechanical allodynia evoked by EtOH (30%, i.pl.) or Veh in *Trpa1*$^{+/+}$ and *Trpa1*$^{-/-}$ mice. (**I**) Dose-dependent acute nociceptive response and (**J**) dose- and time-dependent mechanical allodynia evoked by acetaldehyde (ACD, 1-20 nmol, i.pl.) or Veh in C57BL/6J mice. (**K** and **L**) Acute nociceptive response and time-dependent mechanical allodynia evoked by ACD (20 nmol, i.pl.) or Veh in *Trpa1*$^{+/+}$ and *Trpa1*$^{-/-}$ mice. BL, baseline. Veh is the vehicle of EtOH or ACD. (**A**, **C**, **G**, **I** and **K**) box plots with horizontal lines at the 25th percentile, the median, and the 75th percentile and the vertical lines which extend to the minimum and maximum values; (**B**, **D**, **E**, **F**, **H**, **J** and **L**) mean ± SEM with individual data points overlaid; n=8 mice for each experiment. *P<0.05, **P<0.01, ***P<0.001 vs. Veh, Veh-*Trpv1*$^{+/+}$ and Veh-*Trpa1*$^{+/+}$; §P<0.05, §§§P<0.001 vs. EtOH, EtOH-*Trpv1*$^{+/+}$, EtOH-*Trpa1*$^{+/+}$, ACD and ACD-*Trpa1*$^{+/+}$; one-way (**A**, **C**, **G**, **I** and **K**) or two-way (**B**, **D**, **E**, **F**, **H**, **J** and **L**) ANOVA with Bonferroni post-hoc correction.

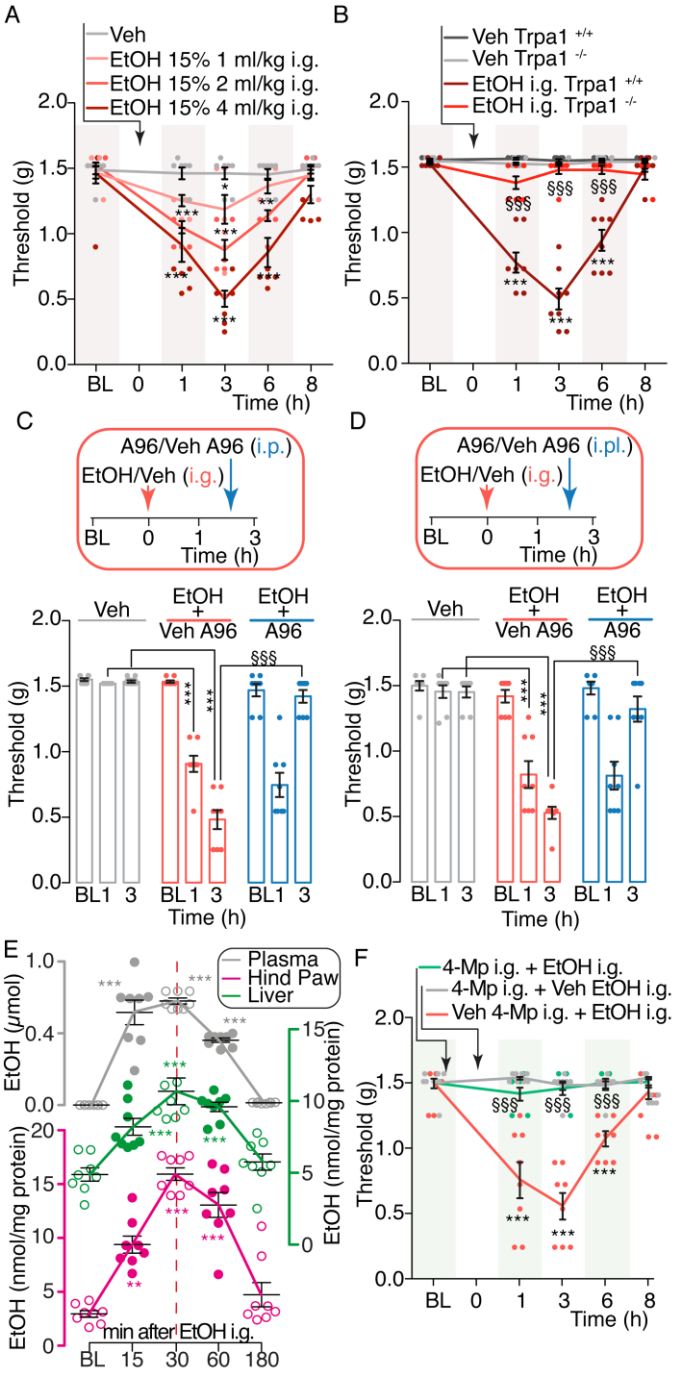

Figure 2. TRPA1 mediates mechanical allodynia evoked by intragastric ethanol in C57BL/6J mice hind paw. (**A**) Dose-dependent mechanical allodynia evoked by ethanol (EtOH, intragastric, i.g.) or vehicle (Veh). (**B**) Time-dependent mechanical allodynia evoked by EtOH (15%, 4 ml/kg, i.g.) or Veh in *Trpa1*$^{+/+}$ and *Trpa1*$^{-/-}$ mice. (**C** and **D**) Mechanical allodynia evoked by EtOH (15%, 4 ml/kg, i.g.) or Veh after A967079 (A96, 100 mg/kg, intraperitoneal, i.p. or 100 µg/site, intraplantar, i.pl.) or Veh A96 in

C57BL/6J mice. (**E**) Time course of EtOH levels in plasma and liver and hind paw tissue, after EtOH (15%, 4 ml/kg, i.g.) in C57BL/6J mice. (**F**) Time-dependent mechanical allodynia evoked by EtOH (15%, 4 ml/kg, i.g.) or Veh in C57BL/6J mice pretreated with 4-methylpyrazole (4-Mp, 50 mg/kg, i.g.) or Veh 4-Mp. BL, baseline. Veh is the vehicle of EtOH. Data are mean ± SEM with individual data points overlaid; n=8 mice for each experimental condition. *P<0.05, **P<0.01, ***P<0.001 vs. Veh and EtOH BL; §§§P<0.001 vs. EtOH-*Trpa1*$^{+/+}$, EtOH-A96 and 4-Mp-EtOH; one-way (**E**) or two-way (**A**-**D** and **F**) ANOVA with Bonferroni post-hoc correction.

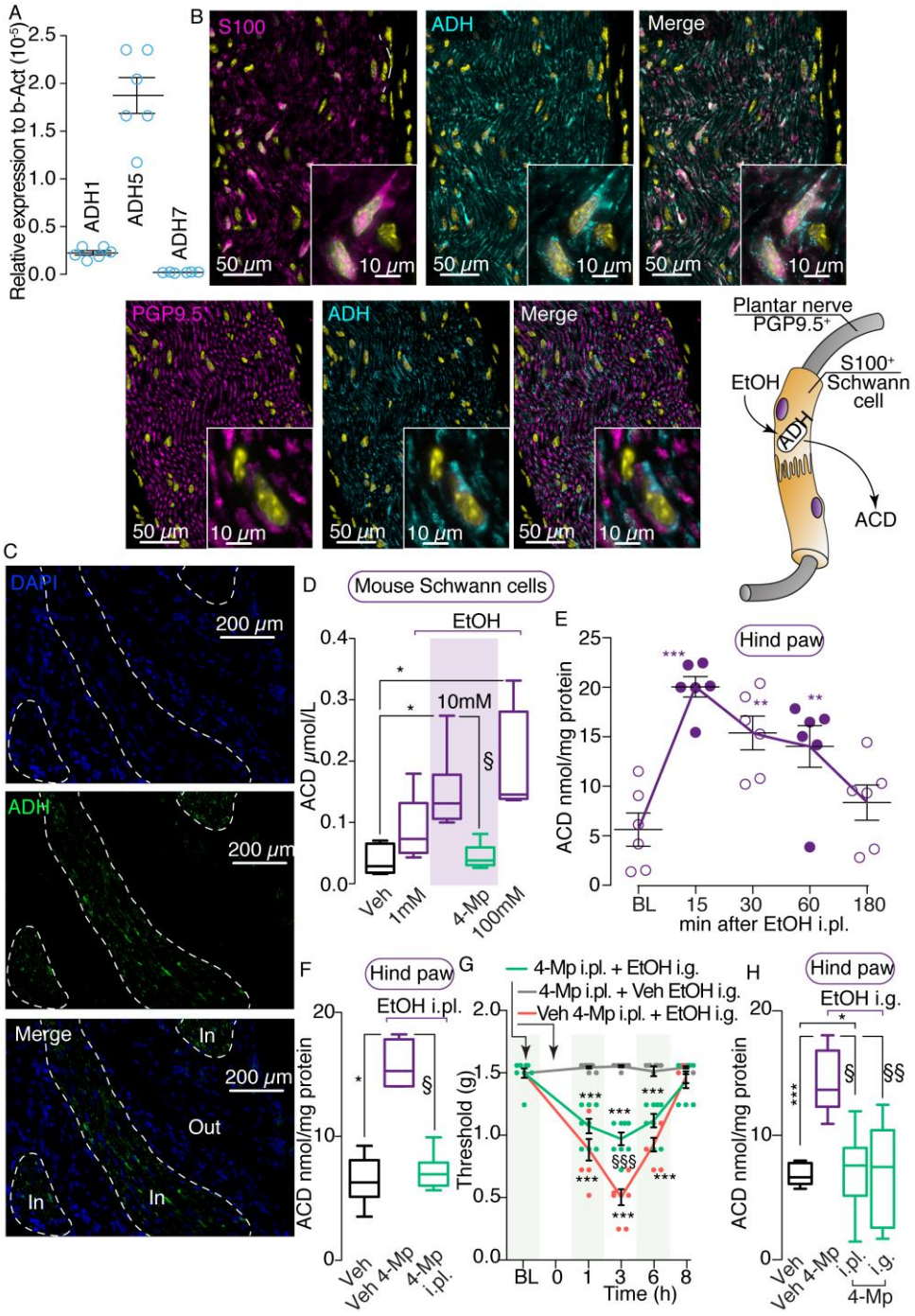

Figure 3. Acetaldehyde is generated by both hepatic and Schwann cell alcohol dehydrogenase. (**A**) Alcohol dehydrogenase (ADH) 1, 5 and 7 (ADH1, ADH5 and ADH7) mRNA relative expression in hind paw tissue in C57BL/6J mice. (**B** and **C**) Representative images of ADH, S100 and PGP9.5 expression in hind paw tissue in C57BL/6J mice. (**D**) Dose-dependent acetaldehyde (ACD) levels in cultured Schwann

cells isolated from C57BL/6J mice and exposed to ethanol (EtOH, 1-100 mM) in the presence of 4-methylpyrazole (4-Mp, 100 µM) or vehicle (Veh 4-Mp). (**E**) Time-dependent ACD levels (hind paw tissue) after intraplantar, (i.pl., 20 µl) EtOH (30%) in C57BL/6J mice. (**F**) ACD levels (hind paw tissue) of C57BL/6J mice receiving EtOH (30%, i.pl.) or Veh and pretreated with 4-Mp (100 µg, i.pl.) or Veh 4-Mp. (**G** and **H**) Time-dependent mechanical allodynia and ACD levels (hind paw tissue) in C57BL/6J mice receiving EtOH (15%, 4 ml/kg, intragastric, i.g.) or Veh and pretreated with 4-Mp (100 µg, i.pl. or 50 mg/kg, i.g.) or Veh 4-Mp. BL, baseline. Veh is the vehicle of EtOH. [In] and [Out] indicate inside and outside, respectively, the *perineurium,* delimited by dashed lines. (**D**, **F** and **H**) box plots with horizontal lines at the 25th percentile, the median, and the 75th percentile and the vertical lines which extend to the minimum and maximum values; (**A**, **E** and **G**) mean ± SEM with individual data points overlaid; n=6-8 mice for each experimental condition. *P<0.05, ***P<0.001 vs. Veh and ACD BL; §P<0.05, §§§P<0.001 vs. EtOH and EtOH-4-Mp; one-way (**D-F**, and **H**) or two-way (**G**) ANOVA with Bonferroni post-hoc correction.

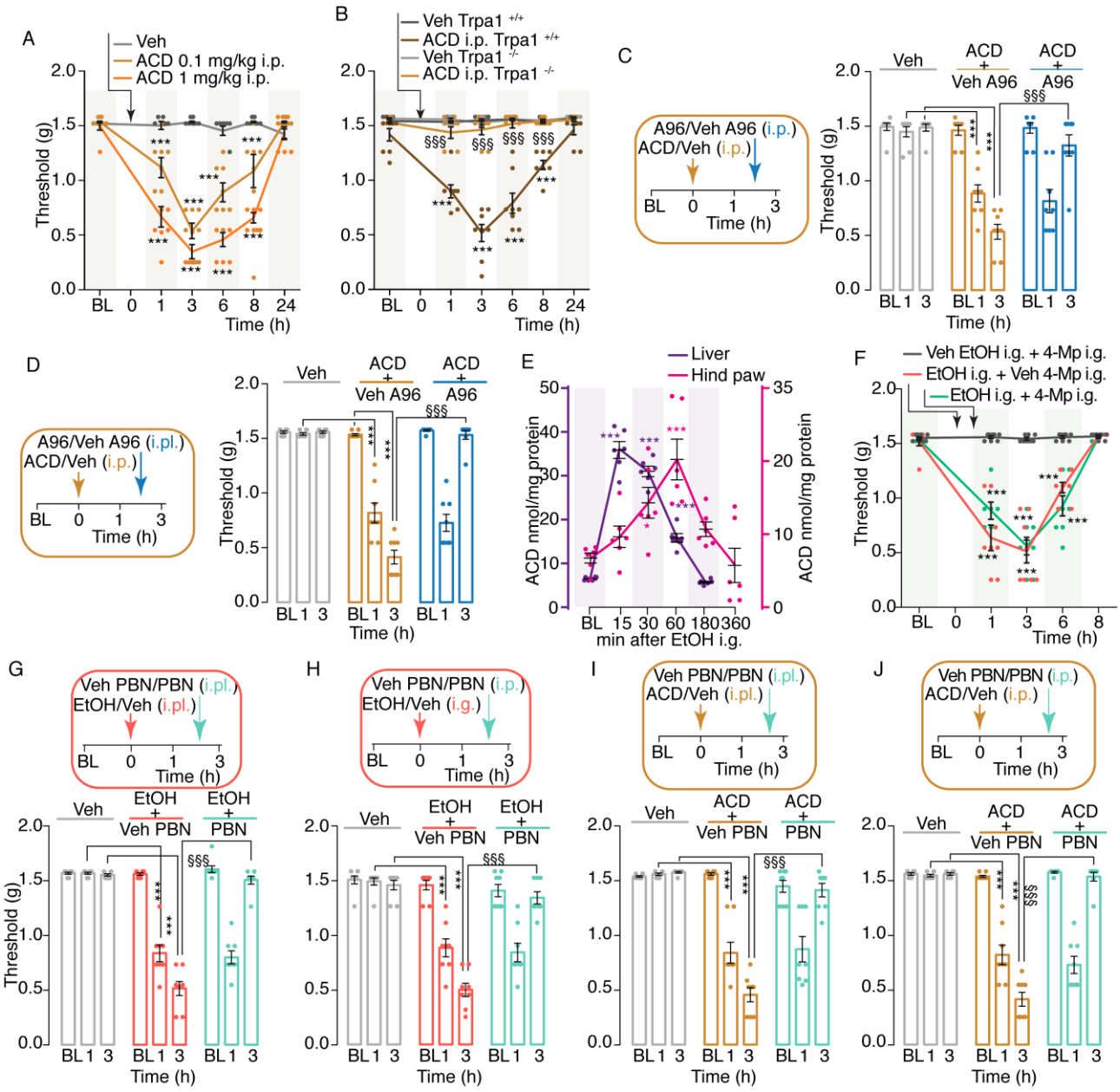

Figure 4. Acetaldehyde *via* TRPA1 sustains ethanol-evoked allodynia in C57BL/6J mice hind paw. (**A**) Dose- and time-dependent mechanical allodynia evoked by acetaldehyde (ACD, intraperitoneal, i.p.) or vehicle (Veh). (**B**) Time-dependent mechanical allodynia evoked by ACD (0.1 mg/kg, i.p.) or Veh in *Trpa1*$^{+/+}$ and *Trpa1*$^{-/-}$ mice. (**C** and **D**) Mechanical allodynia evoked by ACD (0.1 mg/kg, i.p.) or Veh after A967079 (A96, 100 mg/kg, i.p. or 100 µg, intraplantar, i.pl.) or Veh A96 in C57BL/6J mice. (**E**) Time dependent ACD levels in liver and hind paw tissue after ethanol (EtOH,

15%, 4 ml/kg, intragastric, i.g.) in C57BL/6J mice. (**F**) Effect of post treatment with 4-methylpyrazole (4-Mp, 50 mg/kg, i.g.) or Veh 4-Mp on mechanical allodynia evoked by EtOH (15%, 4 ml/kg, i.g.) or Veh, in C57BL/6J mice. (**G** and **H**) Mechanical allodynia evoked by EtOH (30%, i.pl. and 15%, 4ml/kg, i.g.) Veh after phenyl-α-tert-butyl nitrone (PBN, 100 μg, i.pl. or 50 mg/kg, i.p.) or Veh PBN in C57BL/6J mice. (**I** and **J**) Mechanical allodynia evoked by ACD (10 nmol, i.pl. and 0.1 mg/kg, i.p.) or Veh after PBN (100 μg, i.pl. or 50 mg/kg, i.p.) or Veh PBN in C57BL/6J mice. BL, baseline. Veh is the vehicle of EtOH and ACD. Data are mean ± SEM with individual data points overlaid; n=6-8 mice for each experimental condition. *P<0.05, ***P<0.001 vs. Veh and ACD BL; §§§P<0.001 vs. ACD-*Trpa1*$^{+/+}$, ACD-A96, EtOH-PBN and ACD-PBN; one-way (**E**) or two-way (**A-D** and **F-J**) ANOVA with Bonferroni post-hoc correction.

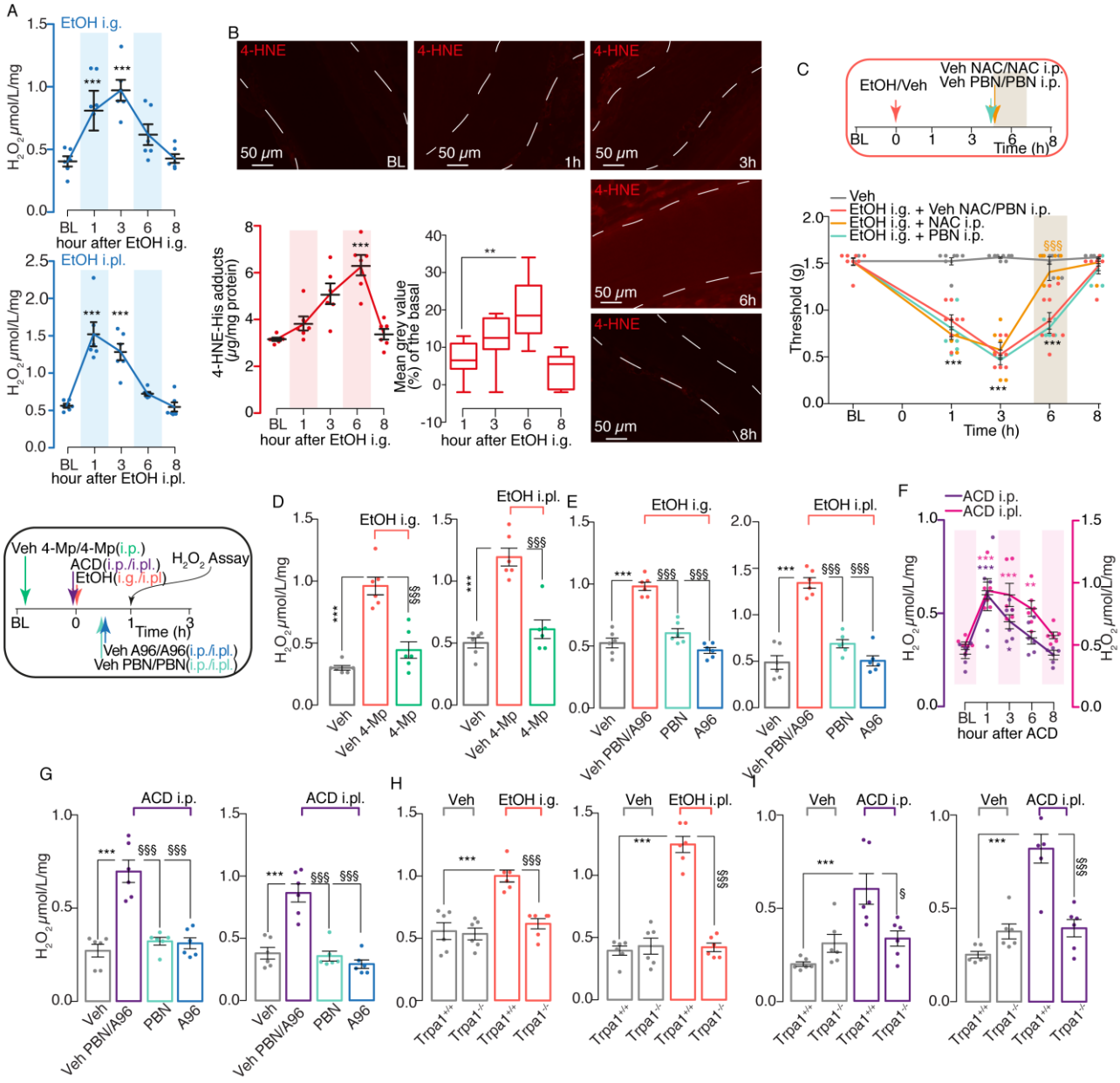

Figure 5. Acetaldehyde *via* TRPA1 generates ROS that sustain ethanol-evoked allodynia. (**A**) H_2O_2 levels (hind paw) after ethanol (EtOH, intragastric, i.g. or intraplantar, i.pl.). (**B**) 4-hydroxynonenal (4-HNE) staining (plantar nerve) and levels (hind paw) after i.g. EtOH (**C**) Mechanical allodynia evoked by EtOH i.g. or vehicle (Veh) after N-acetyl cysteine (NAC, 250 mg/kg, intraperitoneal, i.p.) and phenyl-α-tert-butyl nitrone (PBN, 50 mg/kg, i.p.) or their Veh. H_2O_2 levels (hind paw) after i.g. and i.pl. EtOH or Veh in mice pretreated with (D) 4-methylpyrazole (4-Mp, 50 mg/kg, i.g.), (E) A967079 (A96, 100 mg/kg, i.p.) and PBN (100 mg/kg, i.p.) or their Veh. (**F**) H_2O_2 levels

(hind paw) after acetaldehyde (ACD, 0.1 mg/kg, i.p. or 10 nmol, i.pl.). (**G**) H_2O_2 levels (hind paw tissue) after ACD (0.1 mg/kg, i.p. or 10 nmol, i.pl.) or Veh and pretreated with A96 (100 mg/kg, i.p.) or PBN (100 mg/kg, i.p.) or their Veh . (**H**) H_2O_2 levels (hind paw) in *Trpa1*$^{+/+}$ and *Trpa1*$^{-/-}$ mice treated with (H) i.g. and i.pl. EtOH, (**I**) ACD (0.1 mg/kg i.p. and 10 nmol, i.pl.) or their Veh. BL, baseline. Veh is the vehicle of EtOH and ACD. Where not indicated mice are **C57BL/6J** and EtOH doses are: i.g., 15%, 4 ml/kg and i.pl. 30%, 20 µl. (**B**, 4-HNE mean grey value) box plots with horizontal lines at the 25th percentile, the median, and the 75th percentile and the vertical lines which extend to the minimum and maximum values; all other data are mean ± SEM with individual data points overlaid; n=6-8 mice for each experimental condition. *P<0.05, **P<0.01, ***P<0.001 vs. Veh, ACD-BL and H_2O_2-BL; §P<0.05, §§§P<0.001 vs. EtOH, EtOH-A96, EtOH-PBN, EtOH-*Trpa1*$^{+/+}$, ACD-A96, ACD-PBN and ACD-*Trpa1*$^{+/+}$; one-way (**A**, **B** and **D-I**) or two-way (**C**) ANOVA with Bonferroni post-hoc correction.

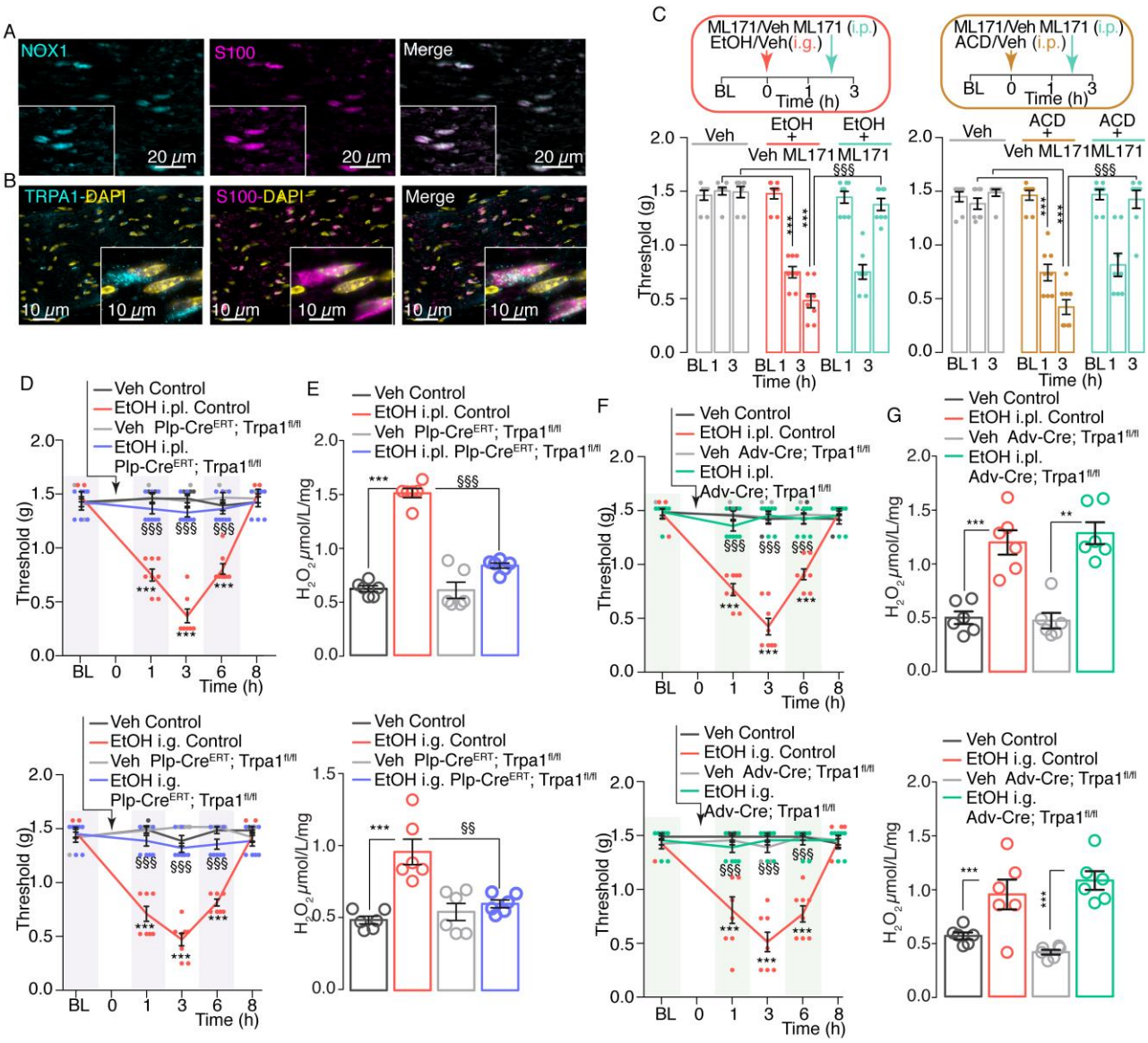

Figure 6. Schwann cell TRPA1 contributes to oxidative stress generation. (**A** and **B**) Representative images of NADPH oxidase 1 (NOX1), S100 and TRPA1 expression in plantar nerve of C57BL/6J mice. (**C**) Mechanical allodynia evoked by ethanol (EtOH, 15%, 4 ml/kg, intragastric, i.g.) and acetaldehyde (ACD, 0.1 mg/kg, intraperitoneal, i.p.) or their vehicle (Veh) after ML171 (100 mg/kg, i.p.) or Veh ML171 in C57BL/6J mice. (**D**) Time-dependent mechanical allodynia evoked by EtOH (30%, intraplantar, i.pl. and 15%, 4 ml/kg, i.g.) or Veh in *Plp-Cre^{ERT};Trpa1$^{fl/fl}$* and *Control* mice. (**E**) H_2O_2 levels (hind paw) after EtOH (30%, i.pl. and 15%, 4 ml/kg i.g.) or Veh in *Plp-Cre^{ERT};Trpa1$^{fl/fl}$* and *Control* mice. (**F**) Time dependent mechanical allodynia evoked

by EtOH (30%, i.pl. and 15%, 4 ml/kg, i.g.) or Veh in *Adv-Cre;Trpa1*$^{fl/fl}$ and *Control* mice. (**G**) H_2O_2 levels (hind paw tissue) after EtOH (30%, i.pl. and 15%, 4 ml/kg, i.g.) or Veh in *Adv-Cre;Trpa1*$^{fl/fl}$ and *Control* mice. BL, baseline. Veh is the vehicle of EtOH and ACD. Dashed lines indicate *perineurium.* Data are mean ± SEM with individual data points overlaid; n=6-8 mice for each experimental condition. **P<0.01, ***P<0.001 vs. Veh; §§P<0.01, §§§P<0.001 vs. EtOH i.g. or EtOH i.pl. control; one-way (**E** and **G**) or two-way (**C, D** and **F**) ANOVA with Bonferroni post-hoc correction.

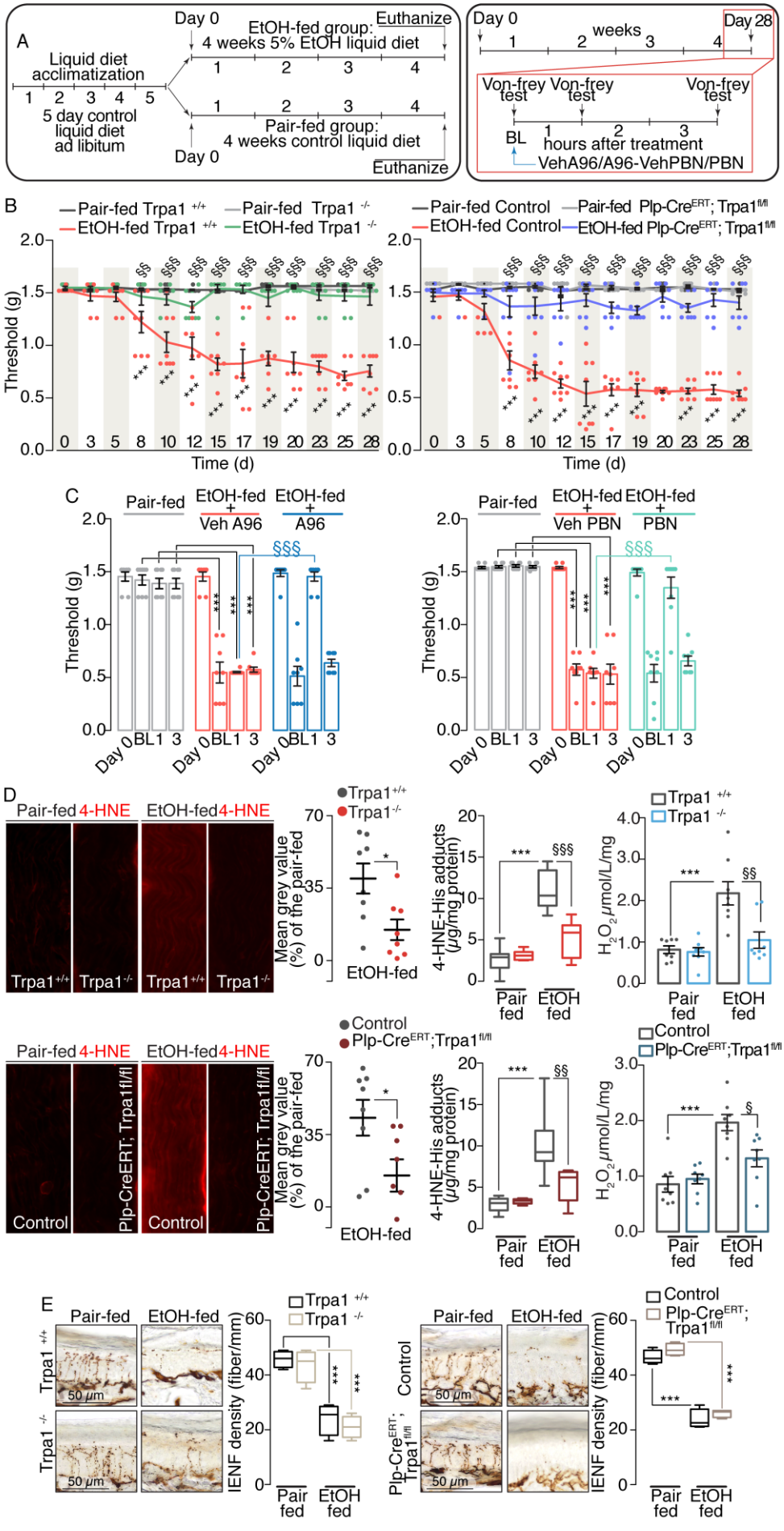
A
Liquid diet acclimatization
5 day control liquid diet ad libitum
Day 0
EtOH-fed group: 4 weeks 5% EtOH liquid diet
Euthanize
Pair-fed group: 4 weeks control liquid diet
Day 0
Euthanize
Day 0
weeks
Day 28
Von-frey test
Von-frey test
Von-frey test
BL
hours after treatment
Veh A96/A96-Veh PBN/PBN
B
Pair-fed Trpa1 +/+
EtOH-fed Trpa1 +/+
Pair-fed Trpa1 -/-
EtOH-fed Trpa1 -/-
Pair-fed Control
EtOH-fed Control
Pair-fed Plp-CreERT; Trpa1fl/fl
EtOH-fed Plp-CreERT; Trpa1fl/fl
Threshold (g)
Time (d)
C
Pair-fed
EtOH-fed + Veh A96
EtOH-fed + A96
EtOH-fed + Veh PBN
EtOH-fed + PBN
Threshold (g)
Day 0 BL 1 3
D
Pair-fed 4-HNE
EtOH-fed 4-HNE
Trpa1+/+
Trpa1-/-
Control
Plp-CreERT; Trpa1fl/fl
Mean grey value (%) of the pair-fed
EtOH-fed
4-HNE-His adducts (µg/mg protein)
H2O2 µmol/L/mg
Pair fed
EtOH fed
E
Pair-fed
EtOH-fed
Trpa1 +/+
Trpa1 -/-
Control
Plp-CreERT; Trpa1fl/fl
50 µm
IENF density (fiber/mm)

Figure 7. Schwann cell TRPA1 mediates mechanical allodynia evoked by chronic ethanol treatment. (A) Overview of the experimental design of the chronic ethanol (EtOH) feeding model. (**B**) Time-dependent mechanical allodynia by EtOH- (5% (vol/vol) for 28 days, EtOH-fed) or control (pair-fed)-diet in *Trpa1*$^{+/+}$ and *Trpa1*$^{-/-}$ mice and *Plp-Cre*^{ERT}*;Trpa1*$^{fl/fl}$ and *Control* mice. (**C**) Mechanical allodynia evoked by EtOH- or control-diet at day 28 after A967079 (A96, 100 mg/kg, intraperitoneal, i.p.) and phenyl-α-tert-butyl nitrone (PBN, 100 mg/kg, i.p.) or their Veh in C57BL/6J mice. (**D**) Representative photomicrographs and cumulative data of 4-hydroxynonenal (4-HNE) staining (plantar nerve) and levels (hind paw), and H_2O_2 levels (hind paw) in *Trpa1*$^{+/+}$ and *Trpa1*$^{-/-}$ mice and *Plp-Cre*^{ERT}*;Trpa1*$^{fl/fl}$ and *Control* mice at day 28 after EtOH- or control-diet. (**E**) Representative photomicrograph of PGP9.5 staining and cumulative data of intraepidermal nerve fiber (IENF) density in the paw of *Trpa1*$^{+/+}$ and *Trpa1*$^{-/-}$ mice and *Plp-Cre*^{ERT}*;Trpa1*$^{fl/fl}$ and *Control* mice at day 28 after EtOH- or control-diet. BL, baseline. (**D**, 4-HNE-His and **E**) box plots with horizontal lines at the 25th percentile, the median, and the 75th percentile and the vertical lines which extend to the minimum and maximum values; all other data are mean ± SEM with individual data points overlaid; n=8 mice for each experimental condition. *P<0.05, ***P<0.001 vs. pair-fed *Trpa1*$^{+/+}$, pair-fed control or EtOH-fed Veh A96/A96 day 0; §P<0.05, §§P<0.01, §§§P<0.001 vs. EtOH-fed *Trpa1*$^{+/+}$, EtOH-fed control or EtOH-fed Veh A96; unpaired two-tailed Student's t-test (**D** mean grey value), one-way (**D** 4-HNE-His adducts and H_2O_2, and **E**) or two-way (**B** and **C**) ANOVA with Bonferroni post-hoc correction.

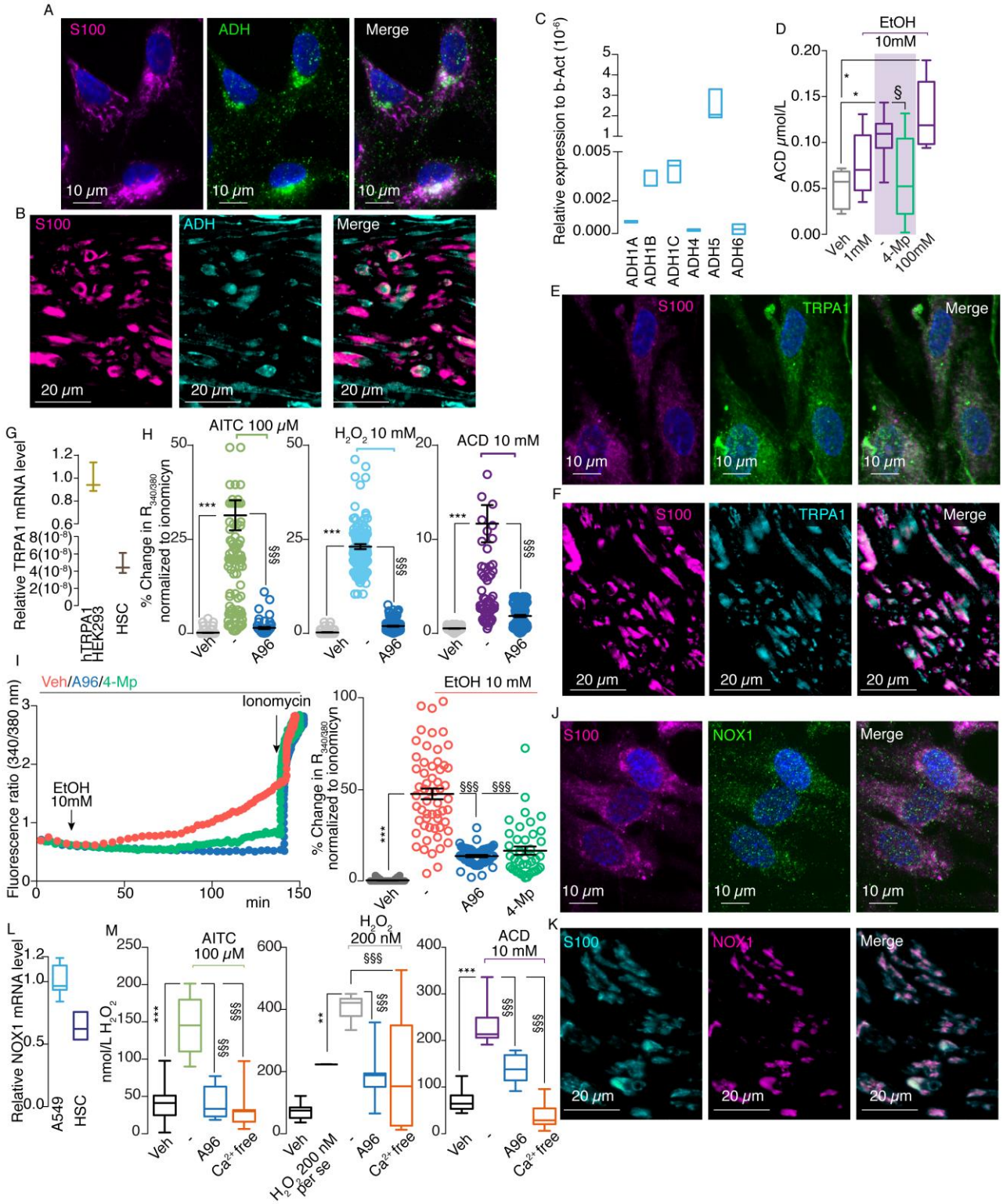

Figure 8. TRPA1 and alcohol dehydrogenase are present in human Schwann cells. Representative images of (**A** and **B**) S100 and alcohol dehydrogenase (ADH) expression, (**E** and **F**) TRPA1 and (**J** and **K**) NOX1 immunofluorescence in cultured

human Schwann cells (HSC) and human skin. (**C**) ADH1A, ADH1B, ADH1C, ADH4, ADH5 and ADH7 mRNA relative expression in HSC. (**D**) Dose-dependent acetaldehyde (ACD) levels in HSC exposed to ethanol (EtOH, 1-100 mM) and treated with 4-methylpyrazole (4-Mp, 100 µM). (**G**) TRPA1 mRNA expression in HSC relative to human TRPA1-HEK293 cells. (**H**) Intracellular calcium ($[Ca^{2+}]_i$) response to allyl isothiocyanate (AITC, 100 µM), H_2O_2 (10 mM) and ACD (10 mM) in HSC in the presence of A967079 (A96, 30 µM) or its vehicle (Veh). (**I**) $[Ca^{2+}]_i$ response to EtOH (10 mM) in HSC in the presence of A96 (30 µM), 4-Mp (100 µM) or their Veh. (**L**) NOX1 mRNA expression in HSC relative to A549 cells. (**M**) H_2O_2 release evoked by AITC (100 µM), H_2O_2 (200 nM) and ACD (10 mM) in HSC in the presence of A96 (30 µM), Veh or in Ca^{2+} free medium. Veh is the vehicle of EtOH, AITC, H_2O_2 and ACD. (**C, D, G, L** and **M)** box plots with horizontal lines at the 25th percentile, the median, and the 75th percentile and the vertical lines which extend to the minimum and maximum values; n=3 replicates from 2 independent experiments in **C, G** and **L** and n=8 replicates from 3 independent experiments in **D** and **M**; **(H** and **I)** data are mean ± SEM with individual data points overlaid, 41 to 327 cells n=3 to 5 experiments. *P<0.05, ***P<0.001 vs. Veh; §P<0.05, §§§P<0.001 vs. EtOH (10 mM), AITC (100 µM), H_2O_2 (200 nM) and ACD (10 mM); (**D, H, I** and **M**) one-way ANOVA with Bonferroni post-hoc correction.